GEOLOGICA CARPATHICA, DECEMBER 2008, 59, 6, 503–514

Stratiform manganese mineralization in the Paleogene and Jurassic shale formations of the Western Carpathians: mineralogy, geochemistry and ore-forming processes

IGOR ROJKOVIČ[1], JÁN SOTÁK[2], PATRIK KONEČNÝ[3] and PETER ČECH[3]

[1]Faculty of Natural Sciences, Comenius University, Mlynská dolina, 842 15 Bratislava, Slovak Republic; rojkovic@cem.sk
[2]Geological Institute of the Slovak Academy of Science, Severná 5, 974 01 Banská Bystrica, Slovak Republic; sotak@savbb.sk
[3]State Geological Institute of Dionýz Štúr, Mlynská dolina 1, 817 04 Bratislava, Slovak Republic; peter.cech@gssr.sk

(Manuscript received May 5, 2008; accepted in revised form September 29, 2008)

Abstract: Manganese mineralization is bound to Paleogene (Oligocene; Rupelian) and Jurassic (Toarcian, Aalenian and Bathonian–Callovian) shales. Mineralization is represented by manganese carbonates (rhodochrosite, kutnohorite and Mn-calcite). Mn-oxyhydroxides (pyrolusite, manganite and rancieite) were formed later during supergene processes by oxidation of manganese carbonates. Paleogene and Jurassic black shales with abundant framboidal pyrite are enriched in organic matter. The average content of organic carbon is 1.04 wt. % in Paleogene shale and 1.11 wt. % in Jurassic shale. The Si/Al ratios of 3.09 in Paleogene shale and 4.04 in Jurassic shale are close to typical marine-sediments and hydrogeneous-detrital manganese accumulations. The distribution of the rare earth elements in the shale suggests continental source and formation in more reducing environment than the Jurassic manganese crusts. Cobalt, copper and nickel contents of mineralized shale are distinctly lower than in oxidic ores in the Jurassic manganese crusts of Western Carpathians. Isotopic composition of calcite in sediments shows positive values $\delta^{13}C$ in most samples of Paleogene and Jurassic carbonates. Increased manganese content in Mn-carbonates is closely associated with distinctly negative values of $\delta^{13}C$ down to –9.9 in Paleogene carbonates and down to –11.2 in Jurassic carbonates. The dominant negative $\delta^{13}C$ composition suggests early-diagenetic origin of Mn-carbonates affected by organic carbon.

Key words: geochemistry, black shale, diagenetic carbonates, supergene oxyhydroxides, C and O isotopes.

Introduction

The origin of manganese deposits is closely related to marine facies and it reflects important events in the geological history of the Earth like transgressions and anoxic events in the ocean (Pratt et al. 1991; Corbin et al. 2000). Mn-oxyhydroxides are deposited in oxic environment of shallow water close to shore while carbonates form in more off-shore environment at reduced conditions of deeper ocean (Roy 1997). Hence, manganese can be sensitive indicator of the oxic-anoxic conditions of the basin.

The manganese mineralization of the Western Carpathians was exploited in the past. Most deposits and occurrences were studied before 1960. The main reason for this study was to provide new data and methods not used before.

The origin of Oligocene manganese ores was explained in terms of re-deposition of clastic or pelitic rocks (Ilavský 1979), chemical precipitation (Munk 1932; Řezáč 1959; Pícha 1964) in an alkaline environment (Pouba 1956) accompanied by biochemical processes (Munk 1932; Řezáč 1959), turbidite currents (Marschalko 1959), and a tectonic activity (Pouba 1956). A possible source of mineralization was lateritic weathering (Pícha 1964), Permian basic volcanic rocks of the Hronic Unit (Ilavský 1950; Cambel 1959), granite of the Nízke and Vysoké Tatry Mts (Munk 1932), and weathered siderite-sulphide deposits of the Spišsko-Gemerské Rudohorie Mts (Marschalko 1959; Řezáč 1959). Alternation of oxidic and carbonate ores was explained in terms of the allogenic origin of oxides and authigenic origin of carbonate, as well as by the recurrent pH and oxic-anoxic conditions (Pícha 1964).

The origin of Jurassic manganese ores near Borinka, Lednické Rovne and Zázrivá was mostly related to sedimentary processes (Polák 1955, 1956, 1957). Despite the low content of organic carbon, mineralization in Branisko was closely related to sedimentation in epicontinental anoxic environment (Polák & Širáňová 1993). The oxidic ore of the Lednické Rovne deposit was attributed to oxidation of primary rhodochrosite (Kantor in Andrusov et al. 1955).

Manganese crusts and nodules, formed during ocean high-stands and corresponding to recent hard grounds, were also found in the Jurassic limestone of the West Carpathian Klippen Belt (Rojkovič et al. 2003a).

Geological setting

The stratiform manganese deposits and occurrences of the Western Carpathians are hosted in the Paleogene, Jurassic and Paleozoic black shale formations (Fig. 1, Table 1). The Paleogene manganese ore occurs in the Central Carpathian Paleogene Basin (CCPB), overlying pre-Tertiary tectonic units south of the Pieniny Klippen Belt. The flysch sediments of the basin are represented mainly by shale and sandstone with conglomerate layers superimposed on the pre-Cenozoic tectonic units of the Inner Carpathians. The CCPB

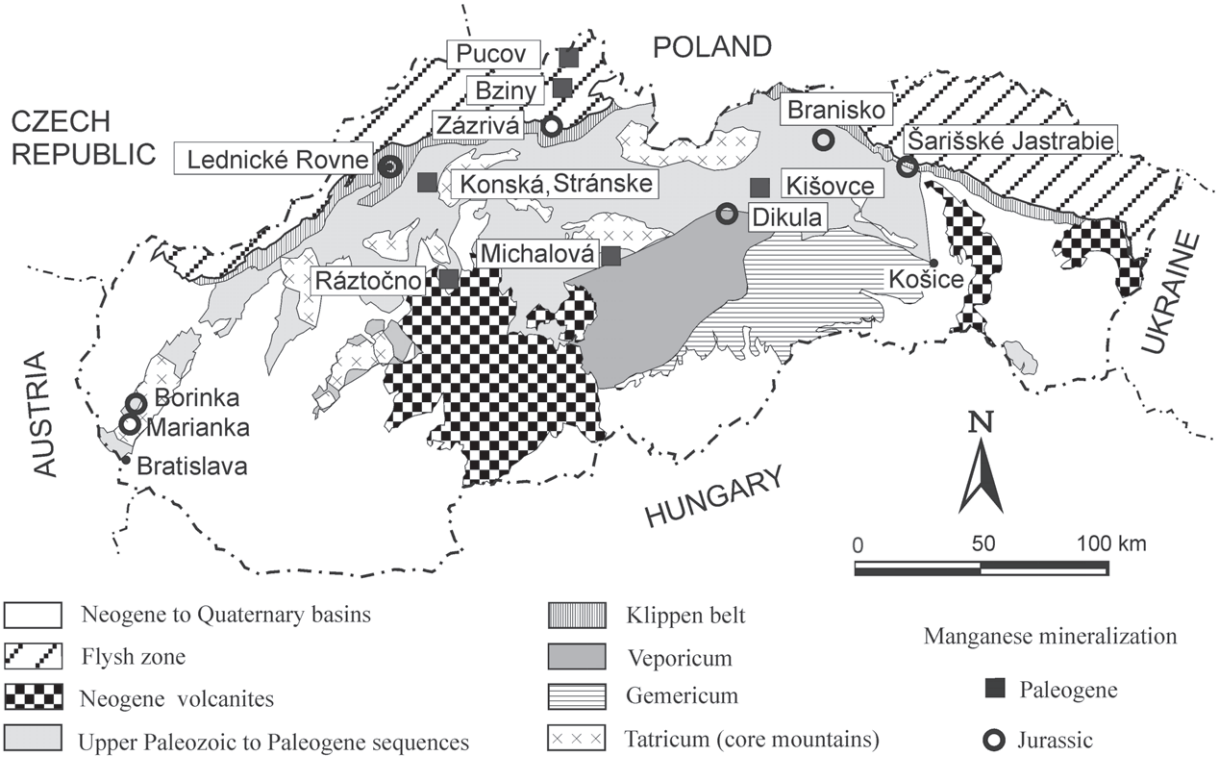

Fig. 1. Deposits and occurrences of the manganese mineralization of the Western Carpathians. GPS locations and a complete list of samples are enclosed in the Electronic Supplement of this paper (Annexes 1 and 2) at www.geologicacarpathica.sk.

Table 1: Stratigraphic position of manganese mineralization in black shales of Western Carpathians.

Period	Epoch	Age	Geological Unit	Locality
Paleogene	Oligocene	Rupelian	Central Carpathian Paleogene	Kišovce-Švábovce, Konská, Stránske, Bziny, Pucov, Michalová
Jurassic	Middle Jurassic	Bathonian–Callovian	Klippen Belt	Šarišské Jastrabie
		Aalenian	Klippen Belt	Lednické Rovne, Zázrivá 2, 3
	Lower Jurassic	Toarcian	Tatricum envelope	Borinka
		Toarcian	Veporicum envelope	Branisko, Dikula
		Toarcian	Krížna Unit	Zázrivá 1

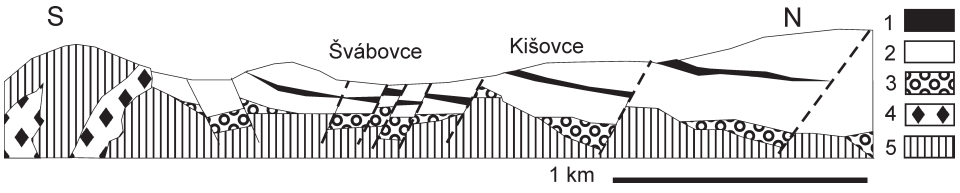

Fig. 2. Geological cross-section of the Kišovce–Švábovce deposit (modified according to Ilavský & Polák 1967). **1** — manganese ore, **2** — Oligocene shale, **3** — Eocene conglomerate, **4** — Permian volcanic rocks, **5** — Permian sediments.

accommodates a subsiding area of a destructive plate-margin (Soták et al. 2001). The manganese layers are bound to a Lower Oligocene sequence (Soták et al. 2001, 2004). Their age is defined by biostratigraphic Zones P18–P19 (*Dentoglobigerina tapuriensis–D. selli*) and NP21–NP23 (*Ericsonia subdisticha–Reticulofenestra ornata*). The position of the manganese layers is equivalent to large manganese deposits of the Eastern Paratethys (Muzylev 1998; Varentsov 2002).

The manganese ore in a horizon up to 3 m thick was mined in the Poprad Basin in the Kišovce-Švábovce area (Fig. 2). Thin bands of oxidic ore with pyrolusite, manganite, marcasite and clay-sandy intercalations alternate here with carbonate bands composed of Mn-calcite, rhodochrosite, pyrite and clay minerals due to rhythmic sedimentation (Konta 1951). The average manganese content varied from 10 to 23 wt. % (Ilavský & Polák 1967). Occurrences of the manganese ore in the Lower Oligocene sequence near Michalová, Konská, Stránske, Bziny, Pucov and Ráztočno villages are less important.

The Jurassic manganese mineralization is related mostly to Toarcian-Aalenian shales. The Toarcian dark grey to black

shale with beds of black sandy crinoid limestone with manganese layers in the lower part are characteristic of the Marianka Formation (Plašienka 1987). The Marianka Formation belongs to the marginal halfgraben on the northern edge of the Tatric Unit and it is analogous to the Lower Austroalpine margin of the Eastern Alps (Plašienka 1987). Its age corresponds to Early to Middle Toarcian according to ammonites and belemnites (Rakús 1994). The Toarcian age based on the structural position and the lithostratigraphic content is presumed also for the grey shale near Dikula (Plašienka 1995) and the Branisko Mts (Polgári et al. 1992; Polák & Širáňová 1993). The manganese mineralization in the black shale of the Klippen Belt is younger. The manganese mineralization is bound to the Skrzypny Formation of Aalenian age near Lednické Rovne and Zázrivá (Wierzbowski et al. 2004), and to the Late Bathonian–Early Callovian Sokolica Formation near Šarišské Jastrabie village (Rojkovič et al. 2003b).

Methods

Outcroping ore layers and surrounding rocks were sampled in rock profiles near Bziny, Dikula, Marianka, Pucov, Šarišské Jastrabie and Zázrivá villages. Other samples were collected from old mining dumps or rare outcrops (Fig. 3).

A total of 120 samples were studied in polished thin sections using polarizing microscope in transmitted and reflected light and scanning electron microscopy (SEM). The carbonates and oxyhydroxides were analysed in the polished thin sections using wave-dispersion X-ray microanalysis (WDX). WDX analyses of Al, Ba, Ca, Fe, K, Mg, Mn, Na, Si and Sr were carried out using a CAMECA SX100 electron microprobe at the State Geological Institute of Dionýz Štúr in Bratislava. The following natural and synthetic standards were used for calibration to calibrate the systems: Al_2O_3, $BaSO_4$, wollastonite, hematite, orthoclase, MgO, rhodonite, albite, SiO_2 and $SrTiO_3$. Operating conditions were: 1–3 μm beam diameter, 15–20 kV accelerating voltage, 19.9–20 nA sample current. Detection limits were better than 0.1 wt. %. The relative standard deviation ranged from ±5 % (for 1 wt. %) to ±25 % (for 0.1 wt. %). The raw data were converted to oxides using PAP correction.

X-ray diffraction (XRD) analysis of a total of 67 samples of separated mineral grains was done on a Phillips PW 1710 diffractometer at the Geological Institute of the Slovak Academy of Science in Bratislava. Samples with a high content of Fe were analysed using Kα irradiation ($\lambda\alpha_1 = 1.78896$ m^{-10}, $\lambda\alpha_2 = 1.79285$ m^{-10}). The CuKα irradiation ($\lambda\alpha_1 = 1.54060$ m^{-10}, $\lambda\alpha_2 = 1.54439$ m^{-10}) was used for other samples. Accelerating voltage 35 kV and beam current 20 mA were used in the range from 4 to 60 °2Θ with 0.02 °2Θ increment.

The chemical composition of a total of 108 rock and ore samples was analysed by atomic emission spectroscopy with inductively coupled plasma (AES-ICP) at Geoanalytical Laboratories of the State Geological Institute of Dionýz Štúr in Spišská Nová Ves. Rare earth elements (REE) were analysed using the same method in a total of 14 samples. Rock-Eval pyrolysis was used to determine organic carbon (TOC) content using the C-MAT STROHLEIN apparatus at the Geological Institute of Slovak Academy of Science in Banská Bystrica in a total of 95 samples.

Carbon and oxygen isotopes were studied in a total of 53 samples. 20 mg of powdered rock was dissolved at 95 °C in phosphorus acid with a density of 1.88 g/cm^3 in a closed reaction vessel (McCrea 1950). The released CO_2 was cleaned in cooling traps and sealed in glass capillary. The $^{13}C/^{12}C$ and $^{18}O/^{16}O$ isotope ratios were measured using a Finnigan MAT 250 mass spectrometer at State Geological Institute of Dionýz Štúr in Bratislava, and expressed as ‰ deviation from V-SMOW (oxygen) and V-PDB (carbon) standards. The oxygen isotope ratio was corrected to the chemical composition of carbonate and the fractionation between CO_2 and H_3PO_4 (Rosenbaum & Sheppard 1986).

Fig. 3. Outcrop of the Paleogene (Rupelian) shale with layer of manganese mineralization (interval with manganese mineralization is marked by arrows; samples By 9.4–9.5 m).

Results

Petrology and mineralogy

The mineralized rocks are represented mainly by shale, in which carbonates, quartz, micas, chlorite and clay minerals are the most abundant phases. The dominant fine-grained carbonates form elongated aggregates or thin layers, parallel to the bedding and thin pyrite layers (Fig. 4). The fine-grained rocks contain parallel oriented quartz, micas and chlorite. Thin sandy intercalations contain fragments of quartz, carbonates, sericite schist, basalt, quartzite, plagioclase and muscovite. Rounded sections of foraminifers, and very rare fragments of coalified plants were also found. Accessory tourmaline, rutile and zircon were common. Carbonates and quartz also form veinlets.

The manganese ores in Oligocene and Jurassic shales are composed of carbonates and oxyhydroxides. The primary minerals are represented by Mn-calcite, kutnohorite and rhodochrosite. The Mn-oxyhydroxides correspond to pyrolusite, rancieite and manganite. The manganese minerals are accompanied by pyrite, marcasite, goethite and iron oxyhydroxides.

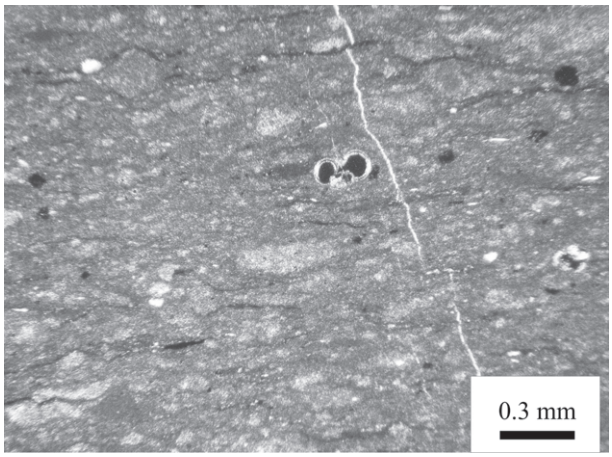

Fig. 4. Oval carbonate aggregates (light), rare quartz fragments (white) and foraminifers (round section) in shale. Kišovce, Kiš-3, transmitted light, parallel nicols.

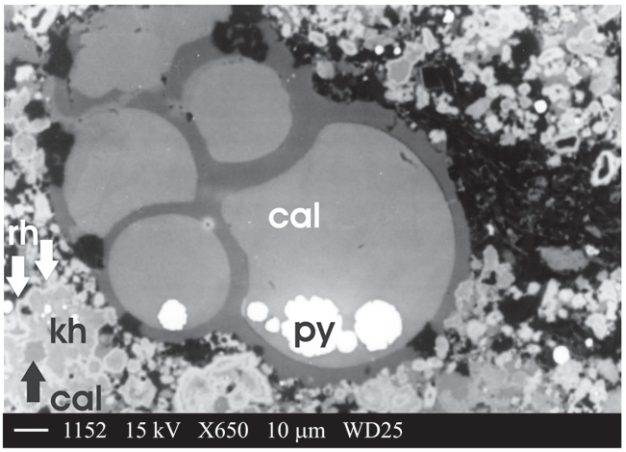

Fig. 6. Calcite (cal) with framboidal pyrite (py) fill foraminifera. Zoned carbonate aggregates are represented by calcite (cal) and kutnohorite (kh) in the centre and by rhodochrosite (rh) in the margin. Kišovce, Kiš-2, SEM-BEI.

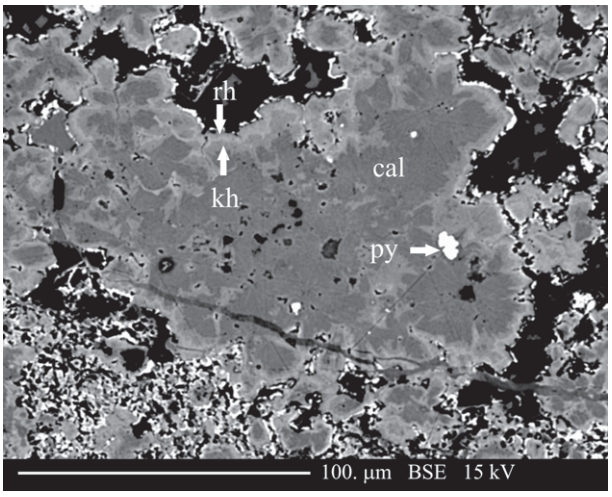

Fig. 5. Zoned carbonates consist of rhodochrosite (rh) on the periphery, kutnohorite (kh) between and calcite (cal) in the centre. Small grains of pyrite (py) are disseminated in the rock. Borinka, Jurassic shale, HN1-6a, SEM, BEI.

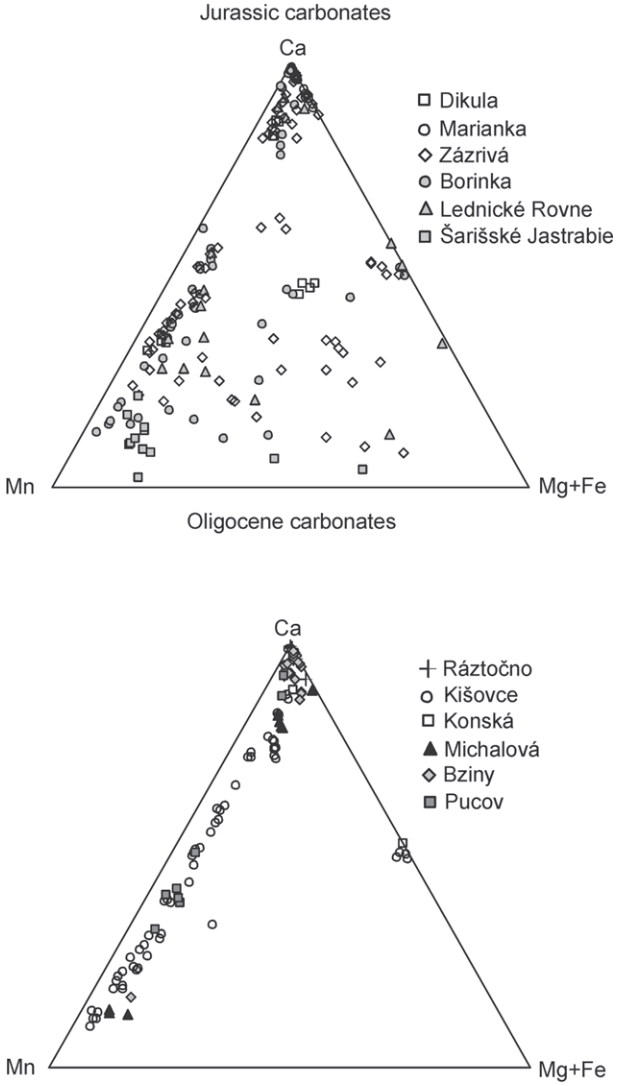

Fig. 7. The chemical composition of carbonates in Oligocene and Jurassic rocks.

The *carbonates* are represented by calcite, Mn-calcite, dolomite, kutnohorite and rhodochrosite. Fine-grained aggregates show zoning in back-scattered electron images. The zoned aggregates are composed of a low-manganese phase in cores and a high-manganese phase in rims. The central part is composed of calcite, Mn-calcite or dolomite and the external part of kutnohorite and rhodochrosite (Fig. 5). These carbonates were also confirmed by X-ray diffraction.

Re-crystallized coarser grained carbonates often fill interiors of foraminifers and radiolarians (Fig. 6). Veinlets of calcite, Mn-calcite and quartz cut older lenticular fine-grained carbonate aggregates.

The carbonates of Jurassic and Paleogene manganese ores show large variability of Ca and Mn contents (Table 2, Fig. 7). The chemical composition of rhodochrosite corresponds to Ca-rhodochrosite. The Mg content reflects the ra-

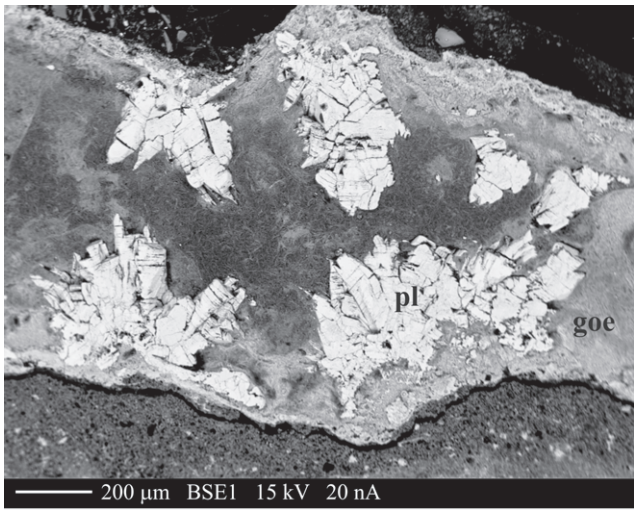

Fig. 8. Aggregate of pyrolusite (pl) in goethite (goe). Borinka, Toarcian shale, BaCDH1, SEM-BEI.

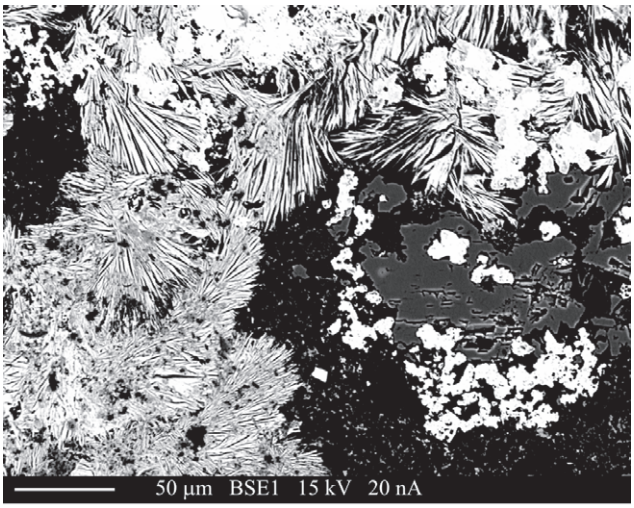

Fig. 9. Radial aggregates of needle-shaped rancieite (light grey) associated with goethite (white). Bziny, Oligocene shale, sample By 9,5b, SEM-BEI.

tio of dolomite fragments observed in the core of carbonate aggregates. Average MgO contents correspond to 2.19 wt. % in the Paleogene ores and 2.38 wt. % of MgO in the Jurassic ores. The Paleogene and the Jurassic carbonates show distinctly different Fe contents. While the average FeO content is 1.13 wt. % in the Paleogene ores, the Jurassic ores are significantly enriched up to 3.93 wt. %. The increased iron content in the Jurassic ores may reflect an enrichment due to mobilization of iron from rock-forming minerals during the Alpine orogeny.

Pyrolusite $Mn^{4+}O_2$ was identified in the reflected light by the highest reflectivity among the manganese minerals, strong anisotropy (yellow–dark brown) and characteristic yellow colour. Elongated grains, 0.01 to 0.1 mm in diameter, are disseminated in rock or they form aggregates with radial texture and veinlets, replacing carbonate minerals (Fig. 8). Pyrolusite also forms thin crusts along fissures and on the surface of rocks. The average chemical composition of analysed pyrolusite (Table 3) corresponds to the formula: $Mn^{4+}_{0.985}Ca_{0.005}Fe^{3+}_{0.004}Mg_{0.003}Si_{0.006}Al_{O.002}O_2$.

Rancieite (Ca, Mn^{2+})$Mn^{4+}{}_4O_9 \cdot 3(H_2O)$ and pyrolusite are the most abundant secondary manganese minerals. Rancieite was firstly described in the Liassic shale of the Branisko Mts by Polgári et al. (1992). Rancieite shows distinct bireflectance

Table 2: Chemical composition of carbonates (WDX analyses in weight %)*.

	Paleogene			Jurassic		
	average	minimum	maximum	average	minimum	maximum
CaO	36.24	5.68	56.40	29.86	0.55	59.42
MgO	2.20	0.11	22.10	2.40	0.00	21.65
FeO	1.12	0.00	6.46	3.92	0.00	32.79
MnO	17.09	0.00	54.59	21.64	0.00	53.74
SrO	0.10	0.00	0.70	0.13	0.00	2.51
BaO	0.01	0.00	0.11	0.01	0.00	0.34
CO_2	42.17	37.39	48.63	41.94	36.61	48.69
Total	98.93			99.90		
n	104			164		

n — number of analyses. ***** — complete list of analyses is involved as Electronic Supplement of this paper (Table 2a,b) at www.geologicacarpathica.sk.

Table 3: Chemical composition of ranciete, pyrolusite and manganite (WDX analyses in weight %)*.

	Ranciete			Pyrolusite			Manganite		
	average	**minimum**	**maximum**	**average**	**minimum**	**maximum**	**average**	**minimum**	**maximum**
MnO_2	79.57	75.69	84.98	98.11	94.72	100.00			
Mn_2O_3							88.83	88.06	89.91
CaO	6.53	2.68	11.40	0.35	0.00	1.70	0.10	0.00	0.25
Fe_2O_3	1.01	0.24	6.82	0.37	0.14	3.09	0.19	0.15	0.23
MgO	0.81	0.00	3.16	0.03	0.00	0.29	0.02	0.00	0.03
SiO_2	0.25	0.00	3.36	0.40	0.07	0.92	0.47	0.21	0.84
Na_2O	0.14	0.00	0.71						
K_2O	0.48	0.08	1.13	0.01	0.00	0.03	0.00	0.00	0.02
BaO	0.06	0.00	0.49	0.00	0.00	0.01	0.00	0.00	0.01
SrO	0.11	0.00	0.30						
Al_2O_3	0.19	0.00	1.83	0.13	0.00	0.41	0.07	0.01	0.21
P_2O_5	0.03	0.00	0.29						
Total	89.55			99.40			89.69		
n	129			44			9		

n — number of analyses. ***** — complete list of analyses is involved as Electronic Supplement of this paper (Table 3a,b,c) at www.geologicacarpathica.sk.

and strong anisotropy (bright yellow–dark grey). Colloform zoned aggregates, as well as needle-shaped radial aggregates fill cavities and fissures in rocks and replace zoned carbonate aggregates (Fig. 9). Their average chemical composition corresponds to the formula: $Mn^{total}_{4.099}\ Ca_{0.521}\ Fe^{3+}_{\ 0.057}\ Mg_{0.090}\ Si_{0.019}Na_{\ 0.020}K_{0.046}Ba_{\ 0.002}Sr_{0.005}Al_{0.017}P_{0.002}O_{9.000}$. Mn^{4+} and Mn^{2+} were not distinguished by WDX and they are involved together as total Mn. X-ray diffraction analysis (XRD) confirmed only the strongest lines of rancieite in a few samples.

Manganite $Mn^{3+}O(OH)$ shows reflectance lower than that of pyrolusite, and strong anisotropy. Aggregates of elongated and isometric grains (0.05 to 0.3 mm in size) fill fissures. Its chemical composition corresponds to the formula: $Mn^{3+}_{1.973}Ca_{0.003}Fe^{3+}_{\ 0.004}Si_{0.014}Al_{0.002}O_3$. Mn^{3+} represents total Mn.

Pyrite FeS_2 forms framboids, spheroids, euhedral grains (0.05 to 2 mm in size), zoned aggregates and thin veinlets. Framboids and re-crystallized spherical grains are frequently disseminated or form clusters. Pyrite grains and aggregates are concentrated into thin bands rarely up to 10 cm thick. Pyrite forms pseudomorphs after foraminifers, replacing and rimming them.

Marcasite FeS_2 forms lath-shaped crystals along fissures in pyrite aggregates.

Goethite α-$Fe^{3+}O(OH)$ and iron oxyhydroxides often intergrow or rim manganese oxyhydroxides. They fill fissures and cavities. They replace or rim carbonates and pyrite. Their chemical composition shows large variability of manganese and iron content due to the close intergrowths of their oxyhydroxides.

Geochemistry of manganese ores

The dominant components of the Jurassic and the Paleogene shale are Al_2O_3, SiO_2 and CaO (Table 4). SiO_2 content in the shale varies from 3.42 to 49.99 wt. % (average 27.60 wt. % in the Paleogene shale and 28.35 wt. % in the Jurassic shale). Al_2O_3 varies from 0.60 to 17.12 wt. % in the shale (average 7.90 wt. % in the Paleogene shale and 6.20 wt. % in the Jurassic shale). The Si/Al ratio corresponds to 3.09 in the Paleogene shale and 4.04 in the Jurassic shale (Fig. 10). The MnO content in the Jurassic manganese ores reaches up to 34.06 wt. % and up to 43.23 wt. % in the Paleogene ores.

The Fe_2O_3 content (total Fe including Fe^{2+} and Fe^{3+}) reaches up to 25.28 wt. % in the Paleogene shale and 35.67 wt. % in the Jurassic shale (average 7.38 wt. % in the Paleogene shale and 8.49 wt. % in the Jurassic shale). The

Table 4: Chemical composition of the Paleogene and Jurassic shale with manganese mineralization (oxides and C in weight %, elements in ppm)*.

	Paleogene shale					Jurassic shale				
	average					average				
	Mn < 1%	Mn > 1%	total	minimum	maximum	Mn < 1%	Mn > 1%	total	minimum	maximum
SiO_2	35.92	23.12	27.60	3.42	49.99	35.93	23.91	28.35	4.55	49.12
TiO_2	0.50	0.31	0.37	0.07	0.7	0.47	0.20	0.30	0.04	0.73
Al_2O_3	10.60	6.38	7.90	1.57	17.12	10.29	3.81	6.20	0.6	15.73
Fe_2O_3total	5.52	8.75	7.38	2.16	25.28	4.64	9.97	8.49	0.98	35.67
MnO	0.43	15.44	8.86	0.04	43.23	0.23	14.41	9.17	0.132	34.06
MgO	2.75	2.31	2.42	0.55	14.91	2.48	3.26	2.97	0.15	9.79
CaO	20.40	17.80	18.30	2.29	39.66	22.36	18.15	19.70	1.31	40.22
Na_2O	0.63	0.34	0.44	0.06	2.37	0.71	0.35	0.48	0.02	1.38
K_2O	2.03	1.17	1.48	0.22	3.3	1.97	0.73	1.19	0.03	5.52
P_2O_5	0.15	0.39	0.28	0.06	2.56	0.15	0.47	0.31	0	2.56
H_2O-	1.49	2.29	1.89	0.08	7.81	0.32	0.98	0.74	0.01	8.5
LOI	20.87	22.70	21.24	11.18	40.28	20.46	23.20	22.19	9.52	38.67
B	19	97	92	10	245	92	75	77	2	357
Ba	335	352	334	20	1354	202	346	293	15	2119
Co	16	29	23	2	88	17	49	37	3	191
Cr	79	72	73	22	155	58	27	39	3	93
Cu	42	34	36	6	82	42	30	34	2	84
La	27	26	26	9	83	22	56	40	9	186
Mo	2	9	9	2	111	2	4	3	2	13
Ni	54	71	62	8	186	47	37	41	4	108
Pb	16	18	16	3	43	27	23	25	6	75
Sr	602	664	619	218	1147	1422	321	779	136	2750
V	121	100	106	27	274	91	55	68	3	253
Y	23	24	23	7	39	22	36	32	10	98
Zr	97	78	89	18	299	74	81	86	10	290
Th	9	9	9	2	17	9	7	8	2	14
U	4	4	4	2	9	3	3	3	2	6
TC	5.32	5.36	5.35	0.12	11.13	5.77	6.46	6.21	0.12	11.62
TOC	0.70	1.17	1.04	0.005	5.27	0.67	1.37	1.11	0.1	4.42
TIC	4.62	4.19	4.31	0	10.93	5.10	5.07	4.67	0.04	11.12
CO_2 carb	16.93	13.46	14.04	0.03	40	18.68	17.08	18.34	7.649	30.27
n	26	36	62			17	19	46		

Fe_2O_3total — total Fe including Fe^{2+} and Fe^{3+}, **LOI** — loss of ignition, **n** — number of analyses, **TC** — total carbon, **TOC** — organic carbon,**TIC** — inorganic carbon. ***** — complete list of analyses is involved as Electronic Supplement of this paper (Table 4a,b) at www.geologicacarpathica.sk.

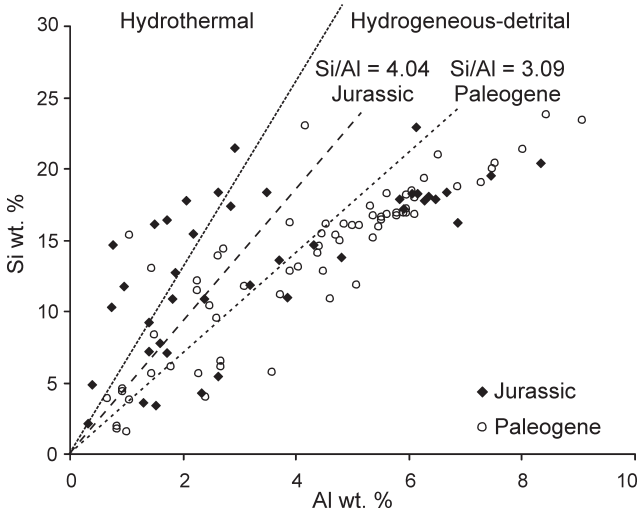

Fig. 10. A plot of Si and Al concentrations, showing an average Si/Al ratio 3.1 for Paleogene shale and 4.0 for Jurassic shale. The boundary between hydrothermal deposits and hydrogeneous detrital sediments according to Crerar et al. (1982).

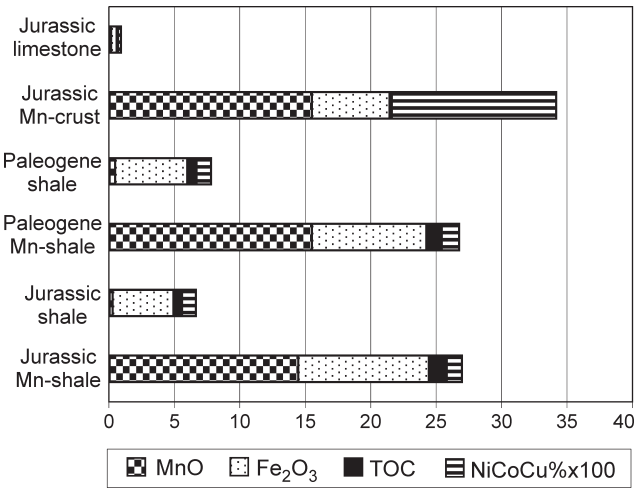

Fig. 11. Average contents of elements and oxides in the studied rocks.

Fe content reflects mostly presence of pyrite and goethite in the manganese ores bound to the Jurassic and the Paleogene shale (Table 4). The Mn/Fe ratio in the Paleogene is 1.33 and in the Jurassic shale is 1.20.

Black and dark grey shales are enriched in organic matter with the average content of organic carbon corresponding to 1.04 wt. % in the Paleogene strata and 1.11 wt. % in the Jurassic strata (Fig. 11).

Trace elements are bound in alumosilicates, carbonates or accessory minerals. V, Cr are related to alumosilicates, Zr, Ti, Th, B to clastic accessory minerals (e.g. rutile, monazite, tourmaline) and Sr to calcite due to isomorphism with Ca. Shales show low contents of Ni, Co and Cu (total 121 ppm in the Paleogene shale and 112 ppm in the Jurassic shale). The rare earth elements (REE) distribution pattern shows only weak positive or absent Ce-anomaly (Figs. 12, 13, Table 5).

Stable isotopes

The stable isotope composition of carbonates reflects variability in their origin and development (Table 6). The carbon isotope composition reflects different formation conditions of carbonates and manganese. Calcite shows $\delta^{13}C$ values close to 0 in Paleogene as well as in Jurassic samples. The Mn-carbonates represented mainly by rhodochrosite and kutnohorite are characterized by more distinct negative $\delta^{13}C$ values (down to –9.9 in the Paleogene shale and –11.2 in the Jurassic shale). The correlation coefficient of $\delta^{13}C$ values to MnO corresponds to –0.76. Negative $\delta^{13}C$ values are characteristic for Mn-carbonates in all stratigraphic levels (Fig. 14).

Discussion

The Central Carpathian Paleogene Basin is related to the maximum of the Early Oligocene transgression, a global anoxic event and the beginning of the isolation of the Paratethys (Soták et al. 2001). The Sinemurian-Toarcian northwest Neotethyan margins with adjacent grabens were filled with deep-water black mudstone and organic-rich shale fa-

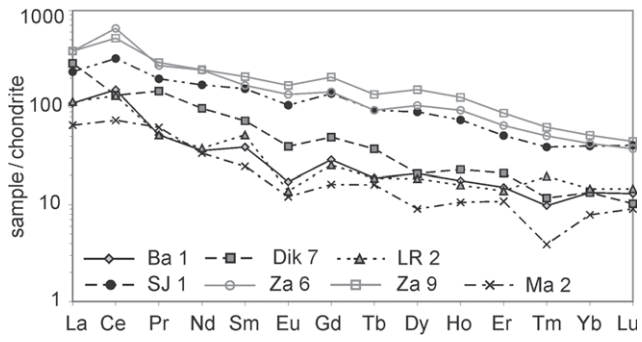

Fig. 12. The distribution pattern of REE in the Jurassic mineralized shale. **Ba** — Borinka, **Dik** — Dikula, **LR** — Lednické Rovne, **Ma** — Marianka, **SJ** — Šarišské Jastrabie, **Za** — Zázrivá potok, **ZaK** — Zázrivá, Kozinská. Chondrite values according to Evensen et al. (1978).

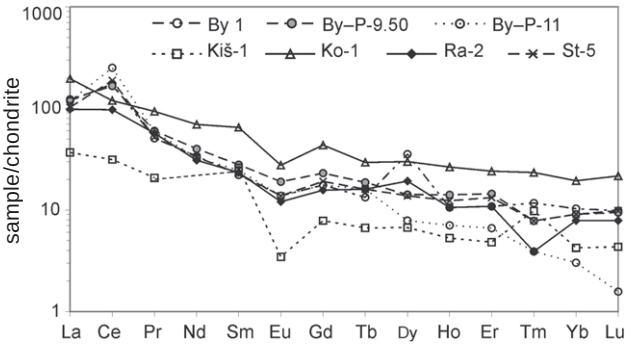

Fig. 13. The distribution pattern of REE in the Oligocene mineralized shale. **By** — Bziny, **Kiš** — Kišovce, **Ko** — Konská, **Ra** — Ráztočno, **St** — Stránske. Chondrite values according to Evensen et al. (1978).

Table 5: REE content in Jurassic and Paleogene mineralized shales (in ppm).

	Jurassic shale with manganese mineralization						
Sample	**Ba 1**	**Dik 7**	**LR 2**	**Ma-P-2m**	**SJ 1**	**Za 6**	**ZaK 9**
Y		59.00	19.00	21.00	18.00	79.00	98.00
La	27.00	70.00	28.00	16.00	57.00	93.00	93.00
Ce	97.00	85.00	84.00	47.00	204.00	417.00	330.00
Pr	5.00	14.20	5.00	6.00	19.00	26.00	28.00
Nd	17.00	46.20	18.00	16.00	81.00	115.00	116.00
Sm	6.00	11.20	8.00	3.80	24.00	26.00	32.00
Eu	1.00	2.30	0.80	0.70	6.10	7.90	9.80
Gd	5.90	10.10	5.20	3.30	28.30	29.50	41.90
Tb	0.70	1.40	0.70	0.60	3.50	3.50	5.10
Dy	5.30	5.30	4.70	2.30	22.80	26.50	38.80
Ho	1.00	1.30	0.90	0.60	4.20	5.30	7.20
Er	2.50	3.50	2.30	1.80	8.50	10.80	14.50
Tm	0.25	0.30	0.50	0.10	1.00	1.30	1.60
Yb	2.20	2.20	2.40	1.30	6.60	7.00	8.50
Lu	0.33	0.26	0.37	0.23	1.03	0.95	1.13
	Paleogene shale with manganese mineralization						
Sample	**By 1**	**By-P-9,50**	**By-P-11**	**Kiš-1**	**Ko-1**	**Ra-2**	**St-5**
Y	31.00	39.00	36.00		37.00	22.00	32.00
La	29.00	30.00	29.00	9.00	48.00	24.00	25.00
Ce	111.00	106.00	160.00	20.00	76.00	62.00	120.00
Pr	4.90	5.80	5.70	2.00	9.00	5.50	5.00
Nd	16.00	18.90	15.40		33.00	14.60	15.70
Sm	3.40	4.30	3.80	4.00	10.00	3.60	3.50
Eu	0.80	1.10	0.80	0.20	1.60	0.70	0.80
Gd	3.60	4.70	3.60	1.60	8.90	3.20	3.90
Tb	0.50	0.70	0.60	0.25	1.10	0.60	0.60
Dy	9.00	3.60	2.00	1.70	7.60	4.90	3.50
Ho	0.60	0.80	0.40	0.30	1.50	0.60	0.70
Er	1.80	2.40	1.10	0.80	4.00	1.80	2.20
Tm	0.30	0.20	0.10	0.25	0.60	0.10	0.20
Yb	1.70	1.50	0.50	0.70	3.20	1.30	1.50
Lu	0.25	0.24	0.04	0.11	0.55	0.20	0.25

Jurassic: Ba — Borinka, Dik — Dikula, LR — Lednické Rovne, Ma — Marianka (non-mineralized shale), SJ — Šarišské Jastrabie, Za — Zázrivá potok, ZaK — Zázrivá Kozinská. **Paleogene:** By — Bziny, Kiš — Kišovce, Ko — Konská, Ra — Ráztočno, St — Stránske.

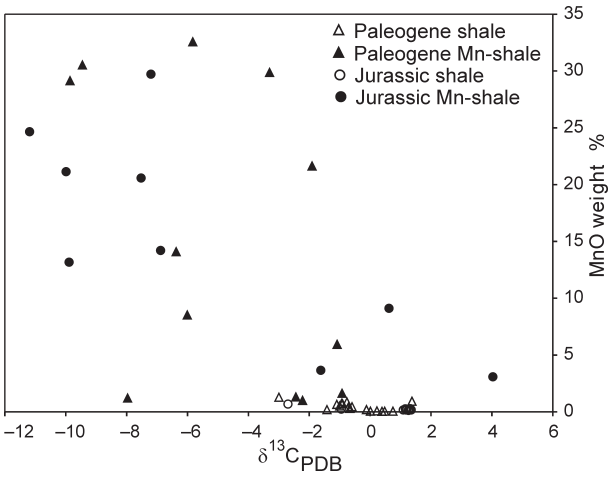

Fig. 14. Correlation of carbon isotope ratios and MnO contents.

cies (Golonka & Ford 2000). Dark grey Toarcian shale with manganese layers in the lower part of the Marianka Formation belongs to marginal halfgraben of the northern edge of the Tatricum and is analogous to the Lower Austroalpine margin of the Eastern Alps (Plašienka 1987). During Toarcian times, the anoxic environment was formed in the Tethys Ocean (Bellanca et al. 1999; Corbin et al. 2000). Manganese horizons related to the black shale were formed in rift basins of the continental margin, occurring recently also in Austria, Germany, Hungary, Italy and Switzerland (German 1972; Cseh-Németh et al. 1980; Jenkyns et al. 1991). The deposits on the margins of black shale facies formed during high sea level stands in narrow time intervals, when ocean anoxia was widespread (Force & Cannon 1988).

The studied Jurassic and Paleogene shales contain abundant carbonate aggregates often elongated along bedding, parallel to thin pyrite layers. The carbonate aggregates are zoned with the central part represented by calcite, Mn-calcite or dolomite and the external part composed of kutnohorite and rhodochrosite. Mn-enrichment in external phases suggests later diagenetic enrichment. Primary rhodochrosite can be formed in a transition zone to deeper sea, under more reducing conditions in shale, sandstone and bituminous shale with pyrite (Borchert 1980).

Pyrite framboids are often concentrated into thin bands or form pseudomorphs after foraminifers, replacing and rimming them. It also suggests formation during diagenesis in a reducing environment. The framboidal texture suggests a diagenetic origin in sense of the "organic globule" model (Rickard 1970). The origin of the framboidal pyrite is associated with consid-

Table 6: Isotopic composition of oxygen and carbon in carbonates of the manganese ores and accompanying rocks.

Sample	Locality	Age	Rock	$\delta^{18}O_{PDB}$	$\delta^{13}C_{PDB}$	$\delta^{18}O_{SMOW}$	MnO
Ba 4	Borinka	Toarcian	marl shale	–7.2	–11.2	23.4	24.66
Ba 5	Borinka	Toarcian	marl shale	–4.7	–10.0	26.1	21.14
Ba 6a,	Borinka	Toarcian	marl shale	–6.2	–1.6	24.5	3.66
ByP 1	Bziny	Oligocene	shale	–4.3	–2.2	26.4	1.00
ByP11, 10	Bziny	Oligocene	shale	–3.7	–1.1	27.0	0.65
ByP 14	Bziny	Oligocene	shale	–7.7	1.4	22.9	0.94
ByP 18	Bziny	Oligocene	shale	–3.8	–0.6	27.0	0.45
ByP 5	Bziny	Oligocene	shale	–6.3	–3.0	24.4	1.28
ByP 7	Bziny	Oligocene	shale	–4.0	–1.0	26.7	0.51
ByP 8	Bziny	Oligocene	shale	–5.0	–2.4	25.7	1.31
ByP 9,5	Bziny	Oligocene	shale	–8.0	–6.4	22.6	14.09
Kiš 1	Kišovce	Oligocene	shale	–2.9	–3.3	27.9	29.88
KišHo1	Hozelec	Oligocene	shale	–3.7	–9.9	27.1	29.15
KišŠv 2	Švábovce	Oligocene	shale	–2.3	–1.9	28.4	21.65
KišŠv 7	Švábovce	Oligocene	shale	–4.0	–5.8	26.3	32.57
LR 3	Lednické Rovne	Aalenian	marl shale	–2.0	4.0	28.8	3.08
Ma 0 m	Marianka	Toarcian	marl shale	–7.4	1.3	23.2	0.16
Ma 1, 5 m	Marianka	Toarcian	limestone	–7.5	1.3	23.1	0.28
Ma P 1 m	Marianka	Toarcian	marl shale	–7.3	1.3	23.3	0.17
Ma P 2	Marianka	Toarcian	marl shale	–4.4	–1.0	26.3	0.23
Ma P 3	Marianka	Toarcian	marl shale	–7.2	1.3	23.4	0.18
Ma P 3, 4	Marianka	Toarcian	limestone	–6.5	1.3	24.1	0.26
Ma P 4	Marianka	Toarcian	marl shale	–7.3	1.3	23.3	0.18
Ma P 5	Marianka	Toarcian	marl shale	–7.4	1.3	23.2	0.19
Ma P 6	Marianka	Toarcian	marl shale	–7.3	1.2	23.3	0.17
Ma P 7	Marianka	Toarcian	marl shale	–7.4	1.3	23.2	0.17
Ma P 8 m	Marianka	Toarcian	marl shale	–7.1	1.3	23.5	0.13
Ma P 8, 10	Marianka	Toarcian	limestone	–7.7	1.2	23.0	0.27
Ma P 9 m	Marianka	Toarcian	marl shale	–7.2	1.1	23.5	0.16
Ma 9.5 m	Marianka	Toarcian	marl shale	–7.5	1.2	23.1	0.21
Mich 11	Michalová	Oligocene	shale	–3.3	–9.5	27.5	30.54
P1	Pucov	Oligocene	marl	–4.3	0.5	26.5	0.06
P2	Pucov	Oligocene	marl	–5.1	0.8	25.7	0.05
P3	Pucov	Oligocene	marl	–5.2	0.2	25.5	0.08
P4	Pucov	Oligocene	marl	–4.4	0.4	26.4	0.04
P5	Pucov	Oligocene	marl	–6.3	0.0	24.4	0.06
P6	Pucov	Oligocene	shale	–4.2	–0.1	26.5	0.20
P7	Pucov	Oligocene	shale	–5.3	–1.4	25.4	0.19
P8	Pucov	Oligocene	shale	–5.0	–0.7	25.8	0.39
P9	Pucov	Oligocene	shale	–5.1	–0.7	25.7	0.31
P10	Pucov	Oligocene	shale	–4.3	–0.9	26.5	0.74
P11	Pucov	Oligocene	shale	–4.4	–0.8	26.3	0.86
P11a	Pucov	Oligocene	shale	–4.1	–8.0	26.7	1.21
P 12a	Pucov	Oligocene	shale	–2.1	–6.0	28.7	8.52
P 13a	Pucov	Oligocene	shale	–4.5	–0.9	26.2	1.63
Ra 1	Ráztočno	Oligocene	shale	–4.2	–0.9	26.5	0.73
Ra 2	Ráztočno	Oligocene	shale	–4.2	–1.1	26.5	5.95
ŠJ 9	Šarišské Jastrabie	Bathonian–Callovian	shale	–1.6	–7.5	29.2	20.59
ŠJ 16	Šarišské Jastrabie	Bathonian–Callovian	shale	–1.9	–7.2	28.9	29.72
Za 1	Zázrivá	Toarcian	marl shale	–5.3	0.6	25.4	9.11
Za 6	Zázrivá	Toarcian	marl shale	–5.2	–9.9	25.5	13.17
ZaH 11	Zázrivá 2	Aalenian	marl shale	–5.4	–2.7	25.3	0.68
ZaH 19	Zázrivá 2	Aalenian	marl shale	–3.4	–6.9	27.3	14.20

erable concentration of hydrogen sulphide derived from decomposition of organic matter or bacterial activity (Kříbek 1977). Honjo et al. (1965) confirmed an influence of gravitation on framboids of the early-diagenetic stage. Concentration of the framboidal pyrite in the bottom of foraminifers is evident (Fig. 6).

The average chemical composition of the Jurassic Western Carpathians manganese ores is similar to the chemical composition of the primary carbonate ores in Alps (German 1972) and to the Úrkút deposit in Hungary (Cseh-Németh et al. 1980). An average Si/Al ratio corresponding to 3.09 in the Paleogene and 4.04 in Jurassic shales are close to marine sediments with an average Si/Al=3 according to Turekian & Wedepohl (1961). The Si/Al ratio is much higher for manganese crusts of hydrothermal origin. Crerar et al. (1982) report on the Si/Al ratio of about 6 for the boundary between hydrothermal and hydrogeneous-detrital manganese accumulations, and the Si/Al ratio of about 35 for manganiferous cherts of the Franciscan assemblage. However, Toth (1980) determined the Si/Al ratio of 5.1 for Fe-Mn crusts of probable hydrothermal origin. The studied samples show larger dispersion of the Si/Al values even in the same locality. A

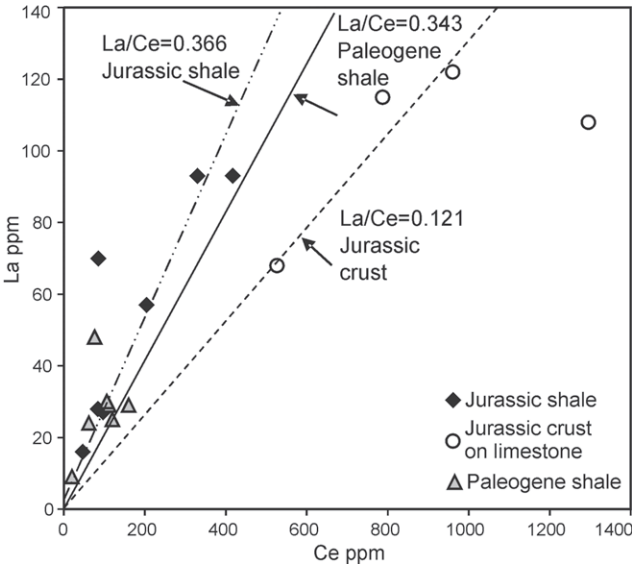

Fig. 15. Correlation of La and Ce in mineralized Jurassic shale and crusts, and in Oligocene shale (modified after Toth 1980).

few samples overlap the field of hydrothermal deposits, but most samples from the same locality are consistent with a hydrogeneous-detrital origin. Increased Si content in some samples may indicate some distal influence of hydrothermal source which was suggested in a Toarcian manganese carbonate-silicate deposit of the Krížna Unit in the Polish Tatra Mountains (Jach & Dudek 2005). The REE distribution is very close to that of manganese ores in the Jurassic shale of the Northern Calcareous Alps (Rantitsch et al. 2003). The REE distribution pattern with absent negative Ce-anomaly suggests sedimentation in seawater and continental sources (Ohta et al. 1999). Distinctly higher La/Ce ratio of manganese ores in the Jurassic (La/Ce = 0.366) as well as in the Paleogene shale (0.343) compared to the manganese crusts on the Jurassic limestone (0.121) suggests reducing conditions of manganese ores hosted in shales (Fig. 15). La/Ce ratio 0.25 was recorded in the sub-marine manganese-iron crusts enriched by Ce^{4+} (Toth 1980). Both types are far away from the La/Ce ratio of 2.8 diagnostic of sea-water and typical of hydrothermal deposits (Nath et al. 1997).

The manganese ores of the Paleogene and Jurassic shales can be distinguished according to 10-times lower content of Ni, Co and Cu compared to the oxidic manganese nodules and crusts on the Jurassic limestone of the Western Carpathians containing up to 1255 ppm (Rojkovič et al. 2003a). Similar low content of Ni, Co, Pb and Cu suggests sedimentation of the manganese ore in a shallow sea (Roy 1980). Mn content is higher than that of iron in the studied ores (average Mn/Fe = 1.33 in the Paleogene shale and 1.20 in the Jurassic shale). This is in agreement with diagenetic origin and sedimentation in a shallow sea. In contrast, higher Mn/Fe, Mn/Co, Mn/Ni, Mn/Cu and Mn/Pb ratios are diagnostic of the open-sea sediments (Roy 1980).

The shales associated with manganese mineralization represent sedimentary rocks enriched with organic matter, with the average content of organic carbon 1.04 wt. % in Paleogene and 1.11 wt. % in Jurassic shales. Oxidic manganese ore in nodules and crusts on the Jurassic limestone showed only 0.20 wt. % of C_{org}. This corresponds to an average content of organic carbon about 2.1 wt. % in the continental shelf and 0.17 wt. % in deep ocean nodules (Manheim 1965). The reducing environment of the Paleogene and Jurassic shales was confirmed by the association of manganese carbonates, the presence of framboidal pyrite and mainly by the increased content of organic carbon.

Manganese carbonates are characterized by distinct negative values of $\delta^{13}C$ (up to –11 ‰) in the Paleogene and Jurassic shales. The negative values of $\delta^{13}C$ in carbonates of the black shale (–9.9 in Paleogene and –11.2 in Jurassic carbonates) are related to increased Mn contents (Fig. 14). The manganese rich carbonates were formed with the distinct assistance of organic carbon.

The isotopic composition is similar to that of the early-diagenetic Lower Oligocene ores at Nikopol in Ukraine with $\delta^{13}C$ values from –4.9 to –26.4 ‰ (Kuleshov 2003). The younger generation of the late-diagenetic (catagenetic) carbonates enriched in ^{12}C is more significantly affected by the organic matter, as known in the Chiaturi and Mangyshlak deposits, where the values of –34.5 and –32.9 m, respectively, have been reported (Kuleshov 2003). Such values have not been determined in the West Carpathian manganese ores. The carbon isotope composition of the studied manganese ores suggests formation during early-diagenetic processes, similar to that in the Nikopol manganese deposit. No significant difference in the oxygen isotopic composition was observed in the studied ores, similar to the Mn ores of the Black Sea coast (Kuleshov 2003).

The early-diagenetic formation of Mn-carbonates resulting from bacterial reduction of manganese in a near-surface environment was confirmed by negative $\delta^{13}C$ values in the Lower Jurassic manganese ore of the Krížna Unit of the Tatra Mountains in Poland (Krajewski et al. 2001). Similarly, Polgári et al. (1991) suggest bacterial reduction during very early burial for the Jurassic manganese carbonates at Úrkút in Hungary. Okita et al. (1988) documented a correlation between $\delta^{13}C$ values and manganese content of carbonates from the Molango deposit in Mexico. The manganese content increased with decreasing $\delta^{13}C$ values from normal seawater values in calcite close to 0 ‰ to as low as –16 ‰ for rhodochrosite. These data were interpreted as those representing manganese reduction via organic matter oxidation (Okita 1992). The manganese ore of the Taoijang deposit in China with negative $\delta^{13}C$ values also suggests biogeochemical enrichment during diagenesis (Fan et al. 1992). More negative $\delta^{13}C$ values in rhodochrosite compared to those in kutnohorite or calcite are similar to the manganese ores of the south-western Taurides in Turkey (Öztrük & Hein 1997).

The above mentioned data suggest an early-diagenetic formation of the studied manganese carbonates in the reducing conditions of black shales. Abundant organic detritus caused reduction of Mn^{4+} and Fe^{3+} to Mn^{2+} and Fe^{2+}, which dissolved in pore water and ascended to the sediment-water boundary (Huckriede & Meischner 1996).

Manganese carbonates were formed due to early-diagenetic microbial reduction of manganese oxides by organic mat-

ter (Okita 1992; Öztürk & Frakes 1995; Roy 1997; Öztürk & Hein 1997; Gutzmer & Beukes 1998; Tang & Liu 1999).

The Mn-carbonates were later replaced by oxyhydroxides during weathering of the primary carbonate mineralization. Hence, they represent secondary mineralization, formed due to the oxidation of primary carbonates, as in the Alps (Beran et al. 1983).

Conclusions

The manganese mineralization of Paleogene and Jurassic shales is bound to horizons with increased content of organic carbon formed in an anoxic environment. The mineralization is represented by manganese carbonates (rhodochrosite, kutnohorite and Mn-calcite). Mn-oxyhydroxides (pyrolusite, manganite and rancieite) were formed later during supergene processes by oxidation of the Mn-carbonates.

The Si/Al ratios are close to marine-sediments and hydrogeneous-detrital manganese accumulations. The distribution of rare earth elements confirms manganese sedimentation in sea from a continental source in a reducing environment. Low Ni, Co and Cu contents, increased organic carbon and isotopic composition suggest early-diagenetic accumulation accompanied by bacterial activity.

The isotopic composition of Paleogene and Jurassic calcite mostly shows positive $\delta^{13}C$ values. Manganese carbonates hosted in shales of the same ages are typical of distinctly negative $\delta^{13}C$ values in all stratigraphic levels. The dominant negative $\delta^{13}C$ values corroborate the early-diagenetic origin of manganese carbonates affected by organic carbon.

Acknowledgments: This study was supported by Project No. 0503 of the Ministry of the Environment of the Slovak Republic and by Project VEGA No. 1/1026/04. We thank E. Harčová for help with isotope analysis. The critical comments of M. Polgári (Institute for Geochemical Research of HAS, Budapest, Hungary), J. Hladil (CAS, Prague, Czech Republic) and an anonymous reviewer significantly improved the manuscript.

References

Andrusov D., Gorek A. & Nemčok A. 1955: Manganese deposits of Slovakia II. Manganese ores of the Klippen Belt and Middle Váh Valley. *Geol. Zbor. SAV VI.*, 1–2, 104–114 (in Slovak).

Bellanca A., Masetti D., Neri R. & Venezia F. 1999: Geochemical and sedimentological evidence of productivity cycles recorded in Toarcian black shales from the Belluno basin, southern Alps, northern Italy. *J. Sed. Res.* 69, 466–476.

Beran A., Faupl P. & Hamilton W. 1983: Die Manganschiefer der Strubbergschichten (Nördliche Kalkalpen, Österreich) — eine diagenetisch geprägte Mangankarbonatvererzung. *Tschermaks Mineral. Petrogr. Mitt.* 31, 175–192.

Borchert H. 1980: On the genesis of manganese ore deposits. In: Varentsov I.M. & Grasselly Gy. (Eds.): Geology and geochemistry of manganese. *Akadémiai Kiadó*, Budapest, Vol. II, 13–44.

Cambel B. 1959: Die metallogenen Hauptprovinzen der Slowakei und die Probleme der Metallogenesis der Westkarpaten. *Wiss. Z. Martin-Luther-Univ. Halle-Wittenberg, Math.-Naturwiss.* 8, 2, 181–196.

Corbin J.C., Person A., Iatzoura A., Ferré B. & Renard M. 2000: Manganese in Pelagic carbonates: indication of major Tectonic events during the geodynamic evolution of a passive continental margin (the Jurassic European Margin of the Tethys-Ligurian Sea). *Paleogeogr. Paleoclimatol. Paleoecol.* 156, 123–138.

Crerar D.A., Namson J., Chyi S., Williams L. & Feigenson M.D. 1982: Manganiferous cherts of the Franciscan Assemblage. I. General geology, ancient and modern analogues, and implications for hydrothermal convection at oceanic spreading centers. *Econ. Geol.* 77, 519–540.

Cseh-Németh J., Konda J., Grasselly Gy. & Szabó Z. 1980: Sedimentary manganese deposits of Hungary. In: Varentsov I.M. & Grasselly Gy. (Eds.): Geology and geochemistry of manganese. *Akadémiai Kiadó*, Budapest, Vol. II, 199–221.

Evensen N.M., Hamilton P.J. & O'Nions R.K. 1978: Rare-earth abundances in chondritic meteorites. *Geochim. Cosmochim. Acta* 42, 1199–1212.

Fan D., Liu T. & Ye J. 1992: The process of formation of manganese carbonate deposits hosted in black shale series. *Econ. Geol.* 87, 1419–1429.

Force E.R. & Cannon W.F. 1988: Depositional model for shallow-marine manganese. Deposits around black shale basins. *Econ. Geol.* 83, 93–117.

German K. 1972: Verbreitung und Entstehung Mangan-reicher Gesteine im Jura der Nördlichen Kalpalken. *Tschermaks Mineral. Petrogr. Mitt.* 17, 123–150.

Golonka J. & Ford S.D. 2000: Pangean (Late Carboniferous–Middle Jurassic) palaeoenvironment and lithofacies. *Palaeogeogr. Palaeoclimatol. Palaeoecol.* 161, 1–34.

Gutzmer J. & Beukes N.J. 1998: The manganese formation of the Neoproterozoic Penganga Group, India — revision of an enigma. *Econ. Geol.* 93, 1091–1102.

Honjo S., Fischer A.G. & Garrison R. 1965: Geopetal pyrite in fine-grained limestones. *J. Sed. Petrology* 35, 480–488.

Huckriede H. & Meischner D. 1996: Origin and environment of manganese-rich sediments within black-shale basins. *Geochim. Cosmochim. Acta* 60, 1399–1413.

Ilavský J. 1950: Geology of Švábovce area. *Geol. Sbor.* 2–3–4, 232–242 (in Slovak).

Ilavský J. 1979: Metallogenése de l'Europe alpine central et du sud-est. *Geol. Ústav D. Štúra*, Bratislava, 1–413.

Ilavský J. & Polák S. 1967: Manganese ores. In: Slávik J. (Ed.): Mineral resources of Slovakia. *Slovenské vydavateľstvo technickej literatúry*, Bratislava, 118–127 (in Slovak).

Jach R. & Dudek T. 2005: Origin of a Toarcian manganese carbonate/silicate deposists from the Krížna Unit, Tatra Mountains, Poland. *Chem. Geol.* 224, 136–152.

Jenkyns H.C., Geczy B. & Marshall J.G. 1991: Jurassic manganese carbonates of central Europe and the Early Toarcian anoxic event. *J. Geol.* 99, 137–149.

Konta J. 1951: Thermical study of the sedimentary manganese rock from Švábovce. *Sbor. Ústř. Úst. Geol.* 18, 601–619 (in Czech).

Krajewski K.P., Lefeld J. & Lacka B. 2001: Early diagenetic processes in the formation of carbonate-hosted Mn ore deposits (Lower Jurassic, Tatra Mountains) as indicated from its carbon isotopic record. *Bull. Polish Acad. Sci.* 49, 13–29.

Kříbek B. 1977: Origin of framboidal pyrite. *Časopis pro mineralogii a geologii* 22, 11–18.

Kuleshov V.N. 2003: Isotopic composition ($\delta^{13}C$, $\delta^{18}O$) and origin of manganese carbonate ores from the Early Oligocene deposits, the Eastern Paratethys. *Chem. Erde* 63, 329–363.

Manheim F.T. 1965: Manganese-iron accumulations in the shallow-marine environment. *Narragensett Marine Lab. Publ.* 3, *Univ. of Rhode Island,* 217–276.

Marschalko R. 1959: Contribution to origin of Mn oxid-carbonate deposit Švábovce in the southern part of Levočské Mts. *Acta Geol. Geogr. Univ. Comen.* 2, 221–230 (in Slovak).

McCrea J.M. 1950: On the isotope geochemistry of carbonates and a paleotemperature scale. *J. Chem. Phys.* 18, 849–857.

Munk R. 1932: Deposit of the manganese ore near Kišovce in Slovakia and its origin. *Prometheus*, Praha, 1–76 (in Czech).

Muzylev N.G. 1998: Upper Eocene and Lower Oligocene nannoplankton. In: Krshennikov V.A. & Akhmetiev M.A. (Eds.): Late Eocene-Early Oligocene geological and biotical events on the territory of the former Soviet Union. Part II. The geological and biotical events. Transactions of the Russian Academy of Sciences Geological Institute. *GEOS*, Moscow, 507, 16–18 (in Russian).

Nath B.N., Plüger W.L. & Roelandts I. 1997: Geochemical constraints on the hydrothermal origin of ferromanganese encrustations from the Rodrigues Triple Junction, Indian Ocean. In: Nicholson K., Hein J.R., Bühn B. & Dasgupta S. (Eds.): Manganese mineralization: geochemistry and mineralogy of terrestrial and marine deposits. *Geol. Soc., Spec. Publ.* 119, 119–211.

Ohta A., Ishii S., Sakakibara M., Mizuno A. & Kawabe I. 1999: Systematic correlation of the Ce anomaly with the Co/(Ni+Cu) ratio and Y fractionation from Ho in distinct types of Pacific deep-sea nodules. *Geochemical J.* 33, 399–417.

Okita P.M. 1992: Manganese carbonate mineralization in the Molango District, Mexico. *Econ. Geol.* 87, 1345–1366.

Okita P.M., Maynard J.B., Spiker E.C. & Force E.R. 1988: Isotopic evidence for organic matter oxidation by manganese reduction in the formation of stratiform manganese carbonate ore. *Geochim. Cosmochim. Acta* 52, 2679–2685.

Öztürk H. & Frakes L.A. 1995: Sedimentation and diagenesis of an Oligocene manganese deposit in a shallow subbasin of the Paratethys: Thrace Basin, Turkey. *Ore Geol. Rev.* 10, 117–132.

Öztrük H. & Hein J.R. 1997: Mineralogy and stable isotopes of black shale hosted manganese ores, Southwestern Taurides, Turkey. *Econ. Geol.* 92, 733–744.

Pícha E. 1964: Manganese ores in the Paleogene of the Central Carpathians and their origin. *Věst. Ústř. Úst. Geol.* 39, 4, 251–258 (in Czech).

Plašienka D. 1987: Lithologic-sedimentologic and paleotectonic character of Borinka Unit in the Malé Karpaty Mts. *Miner. Slovaca* 19, 3, 217–230 (in Slovak).

Plašienka D. 1995: Cleavages and folds in changing tectonic regimes: the Veľký Bok Mesozoic Cover Unit of the Veporicum (Nízke Tatry Mts., Central Western Carpathians). *Slovak Geol. Magazine* 1, 2, 92–113.

Polák S. 1955: Primary manganese ore in the Lednické Rovne deposit. *Geol. Práce, Zpr.* 2, 48–59 (in Slovak).

Polák S. 1956: Zázrivá. Final report on exploration in 1953, 1954 and 1955; Manuscript. *Geofond*, Bratislava, 1–112 (in Slovak).

Polák S. 1957: Manganese ores of the Malé Karpaty Mts. *Geol. Práce*, *Zošit* 47, 39–83 (in Slovak).

Polák M. & Širáňová V. 1993: Manganese mineralization in the Liassic cabonate sediments of Branisko Mts. *Geol. Práce, Spr.* 97, 47–51.

Polgári M., Okita P.M. & Hein J.R. 1991: Stable isotope evidence for the origin of the Úrkút manganese ore deposit, Hungary. *J. Sed. Petrology* 61, 384–393.

Polgári M., Molák B. & Surová E. 1992: An organic geochemical study to compare Jurassic black shale-hosted manganese carbonate deposits: Úrkút, Hungary, and Branisko Mountains, east Slovakia. *Explor. Mining Geol.* 1, 63–67.

Pouba Z. 1956: Manganese ores in Czechoslovakia. In: Symposium sobre yacimientos de manganese, 20. *Congreso Geologico International Mexico* 5, 19–23.

Pratt L.M., Force E.R. & Pomerol B. 1991: Coupled manganese and carbon-isotopic events in marine carbonates at the Cenonian-Turonian boundary. *J. Sed. Petrology* 61, 370–383.

Rakús M. 1994: Revision of ammonites from Marianka shales. *Miner. Slovaca* 2, 118–5.

Rantitsch G., Melcher F., Meisel Th. & Rainer Th. 2003: Rare earth, major and trace elements in Jurassic manganese shales of the Northern Calcareous Alps: hydrothermal versus hydrogeneous origin of stratiform manganese deposits. *Miner. Petrology* 77, 109–127.

Rickard D.T. 1970: The origin of framboids. *Lithos* 3, 269–293.

Rojkovič I., Aubrecht R. & Mišík M. 2003a: Mineral and chemical composition of manganese hardgrounds in Jurassic limestones of the Western Carpathians. *Geol. Carpathica* 54, 5, 317–328.

Rojkovič I., Ožvoldová L. & Sýkora M. 2003b: Manganese mineralization near Šarišské Jastrabie. *Slovak Geol. Magazine* 9, 51–64.

Rosenbaum J. & Sheppard S.M. 1986: An isotopic study of siderites, dolomites and ankerites at high temperatures. *Geochim. Cosmochim. Acta* 50, 1147–1150.

Roy S. 1980: Genesis of sedimentary manganese formations. Processes and products in recent and older geological ages. In: Varentsov I.M. & Grasselly Gy. (Eds.): Geology and geochemistry of manganese. *Akadémiai Kiadó*, Budapest, Vol. II, 13–44.

Roy S. 1997: Genetic diversity of manganese deposition in the terrestrial geological record. In: Nicholson K., Hein J.R., Bühn B. & Dasgupta S. (Eds.): Manganese mineralization: geochemistry and mineralogy of terrestrial and marine deposits. *Geol. Soc. Spec. Publ., London* 119, 5–27.

Řezáč B. 1959: Hydrogeological study of mining area Švábovce-Kišovce near Poprad. *Věst. Ústř. Úst. Geol.* 34, 2, 99–107 (in Czech).

Soták J., Pereszlenyi M., Marschalko R., Milička J. & Starek D. 2001: Sedimentology and hydrocarbon habitat of the submarine-fan deposits of the central Carpathian Paleogene Basin (NE Slovakia). *Mar. Petrol. Geol.* 18, 87–114.

Soták J., Majdová M. & Starek D. 2004: Biostratigraphic determination of the Eocene/Oligocene boundary in section Pucov — its effect on age interpretation of the Pucov Conglomerate and sedimentary rocks of the Palaeogene Central Carpathian basin. *Miner. Slovaca* 36, 2, 24 (in Slovak).

Tang S.Y. & Liu T.B. 1999: Origin of the early Sinian Minle manganese deposit, Hunan Province, China. *Ore Geol. Rev.* 15, 71–78.

Toth J.R. 1980: Deposition of submarine crusts rich in manganese and iron. *Bull. Geol. Soc. Amer.* 91, 44–54.

Turekian K.K. & Wedepohl K.H. 1961: Distribution of the elements in some major units of the earth's crust. *Bull. Geol. Soc. Amer.* 12, 175–191.

Varentsov I.M. 2002: Genesis of the Eastern Paratethys manganese ore giants: impact of events at the Eocene/Oligocene boundary. *Ore Geol. Rev.* 20, 65–82.

Wierzbowski A., Aubrecht R., Krobicki M., Matyja B.A. & Schlögl J. 2004: Stratigraphy and palaeographic position of the Jurassic Czertezik Succession, Pieniny Klippen belt (Western Carpathians) of Poland and Eastern Slovakia. *Ann. Soc. Geol. Polon.* 74, 237–256.

Annexe 1: Localization of stratiform manganese mineralization of the Western Carpathians.

Locality	Description	Longitude	Latitude
Borinka — Pod Zámčiskom	Gamekeeper's lodge, E of Borinka village, 200 m N old mining works	17º06´29´´ 17º06´31´´	48º15´20´´ 48º15´24´´
Borinka — Červený domček	3.5 km N of Borinka village, 50 m E of source Červený domček	17º04´55´´	48º17´46´´
Borinka — Lipníky	6.5 km NNE from Borinka village, 5.5 km ESE from Lozorno village, 800 m NE of Lipníky dam	17º06´58´´	48º18´59´´
Bziny	Area "Ohrady", 1 km SE of the church in Bziny village, outcrop	19º19´50´´	49º13´22´´
Kišovce — (Hozelec)	500 m E of eastern margin of Gánovce village. Dump 300 m S of ground elevation 700.9 and 100 m NE of travertine occurrence	20º20´19´´	49º01´40´´
Kišovce — (Hôrka)	900 m N of road Poprad — Spišská Nová ves, dump W of mining building	20º23´19´´	49º01´07´´
Konská	200 m WSW from the church in Konská village	18º41´21´´	49º06´46´´
Lednické Rovne	W of Lednické Rovne village, 750 m NW of St. Anna church and 500 m SW from Sedlačka hill 387.3 m. Old mining works	18º14´42´´	49º05´34"
Mariánka	Outcrop 1.4 km ENE from church in Marianka village	17º04´25´´	48º15´01´´
Michalová	Kubická, dump of "New adit", 30 m S of brook, 100 m NE of railway	19º45´38´´	48º46´32´´
Michalová	Kubická, dump of "Manganese adit" N of brook and 200m NNE of "New adit", 250 m NE of railway	19º45´32´´	48º46´34´´
Pucov	Outcrop 600 m N of Pucov village, 500 m SE of Muráň hill 719.5 m	19º22´51´´	49º13´24´´
Ráztočno	Outcrop NE of village Ráztočno 150 m	18º46´15´´	48º46´18´´
Stránske	20 m W of SW margin of cemetery in Stránske village, fragments in field-path	18º41´59´´	49º06´58´´
Šarišské Jastrabie	Outcrop in Vesné brook, 200 m E of Šarišské Jastrabie, 150 m NNW of ground elevation 605.5 m	20º55´32´´	49º14´28´´
Švábovce	Dump, on SE margin of abandoned mining plant	20º22´12´´	49º02´06´´
Zázrivá 1, Zázrivská dolina	Outcrop on the eastern bank of Zázrivá Brook, 5.5 km S of the church in Zázrivá village	19º09´39´´	49º13´42´´
Zázrivá 2 — Kozinská	Dump, 250 m E of Zázrivá village, 500 m NW of the Hryzeň hill 779.8 m	19º11´49´´	49º17´32´´
Zázrivá 3 — Havrania	Dump, 500 m SE from cross-road in Havrania village	19º11´27´´	49º17´45´´

Annexe 2: List of samples. Part 1 from 3.

No.	Locality	No. of Sample	Source	Description	Results		
					polished thin section (TS)	AES-ICP (ICP)	C, REE
1	Borinka-Pod Zámčiskom	Ba1	dump	Mn ore	TS	AES-ICP	C, REE
2	Borinka-Pod Zámčiskom	Ba4	dump	Mn ore	TS	AES-ICP	C
3	Borinka-Červený domček	Ba5	dump	Mn ore	TS	AES-ICP	C
4	Borinka (Lozorno-Lipníky)	Ba6a	dump	Mn ore	TS		
5	Borinka (Lozorno-Lipníky)	Ba6b	dump	Mn ore	TS	ICP	C
6	Borinka-Červený domček	BaČD1	dump	Mn ore	N,TS		
7	Borinka-Červený domček	BaČD5	dump	Mn ore	TS		
8	Borinka-Červený domček	BaČD7	dump	Mn ore	TS		
9	Červený domček, Mn pingy, 70 m E, of source	BaČD8	dump	Mn-ore	TS		
10	Červený domček, Mn old mine-works, 70 m E of source	BaČD9	dump	Mn-ore	TS		
11	Borinka-Červený domček	BaČD H14	dump	Mn ore		AES-ICP	C
12	Borinka-Červený domček	BaČD H29	dump	Mn ore		AES-ICP	C
13	Borinka-Pod Zámčiskom	BaHN 6A	dump	Mn ore		AES-ICP	C
14	Borinka-Pod Zámčiskom	BaHR26	dump	Mn ore	TS		
15	Borinka-Pod Zámčiskom	BaHR28	dump	Mn ore	TS		
16	Borinka (Lozorno-Lipníky)	BaL4	dump	Mn ore	TS	AES-ICP	C
17	Borinka (Lozorno-Skala)	BaSA 4	dump	Mn ore		AES-ICP	C
18	Bziny	By 1	outcrop	Mn ore	TS3x	ICP	C, REE
19	Bziny, profil, 1 km SE from church, field path	By-P-O	outcrop	marl shale		AES-ICP	C
20	Bziny, profile, 1 km SE from church, field path	By-P-1	outcrop	marl shale	TS	AES-ICP	C
21	Bziny, profile, 1 km SE from church, field path	By-P-2	outcrop	marl shale		AES-ICP	C
22	Bziny, profile, 1 km SE from church, field path	By-P-3	outcrop	marl shale		AES-ICP	C
23	Bziny, profile, 1 km SE from church, field path	By-P-4	outcrop	marl shale		AES-ICP	C
24	Bziny, profile, 1 km SE from church, field path	By-P-5	outcrop	marl shale	TS	AES-ICP	C
25	Bziny, profile, 1 km SE from church, field path	By-P-6	outcrop	marl shale		AES-ICP	C
26	Bziny, profile, 1 km SE from church, field path	By-P-7	outcrop	marl shale	TS	AES-ICP	C
27	Bziny, profile, 1 km SE from church, field path	By-P-8	outcrop	sandy shale	TS	AES-ICP	C
28	Bziny, profile, 1 km SE from church, field path	By-P-9	outcrop	marl shale		AES-ICP	C
29	Bziny, profile, 1 km SE from church, field path	By-P-9,40	outcrop	marl shale with Mn oxides	TS	AES-ICP	C,
30	Bziny, profile, 1 km SE from church, field path	By-P-9,50	outcrop	marl shale with Mn oxides		AES-ICP	C, REE
31	Bziny, profile, 1 km SE from church, field path	By-P-10	outcrop	marl shale		AES-ICP	C
32	Bziny, profile, 1 km SE from church, field path	By-P-11	outcrop	marl shale with Mn oxides	TS	AES-ICP	C, REE
33	Bziny, profile, 1 km SE from church, field path	By-P-11,10	outcrop	marl shale	TS	AES-ICP	C
34	Bziny, profile, 1 km SE from church, field path	By-P-12	outcrop	marl shale		AES-ICP	C
35	Bziny, profile, 1 km SE from church, field path	By-P-13	outcrop	marl shale		AES-ICP	C
36	Bziny, profile, 1 km SE from church, field path	By-P-14	outcrop	marl shale	TS	AES-ICP	C
37	Bziny, profile, 1 km SE from church, field path	By-P-15	outcrop	marl shale		AES-ICP	C
38	Bziny, profile, 1 km SE from church, field path	By-P-16	outcrop	marl shale		AES-ICP	C
39	Bziny, profile, 1 km SE from church, field path	By-P-17	outcrop	marl shale		AES-ICP	C

Explanations: TS — polished thin section, V — thin section, AES-ICP — atomic emission spectroscopy with induction coupled plasma, C — rock-Eval pyrolysis for organic carbon, REE — rare earth elements analysed by atomic emission spectroscopy with induction coupled plasma.

Annexe 2: *Continued*. Part 2 from 3.

No.	Locality	No. of Sample	Source	Description	Results		
					polished thin section (TS)	AES-ICP (ICP)	C, REE
40	Bziny, profile, 1 km SE from church, field path	By-P-18	outcrop	marl shale		AES-ICP	C
41	Bziny, profile, 1 km SE from church, field path	By-P-19	outcrop	marl shale		AES-ICP	C
42	Bziny, profile, 1 km SE from church, field path	By-P-20	outcrop	marl shale		AES-ICP	C
43	Dikula, Baniská	Dik 1	outcrop	Mn ore		AES-ICP	C
44	Dikula, Baniská	Dik 2	outcrop	Mn ore		AES-ICP	C
45	Dikula, Baniská	Dik 3	outcrop	Mn ore		AES-ICP	C
46	Dikula, Baniská	Dik 4	outcrop	Mn ore		AES-ICP	C
47	Dikula, Baniská	Dik 5	outcrop	Mn ore		AES-ICP	C
48	Dikula, Baniská	Dik 6	outcrop	Mn ore		AES-ICP	C
49	Dikula, Baniská	Dik 7	outcrop	Mn ore		AES-ICP	C, REE
50	Kišovce (Hozelec)	Ho 1	dump	Mn ore	TS		C
51	Kišovce (Hozelec)	Ho 2	dump	sandstone	TS	ICP	C
52	Kišovce (Hozelec)	Ho 3	dump	Mn ore	TS	ICP	C
53	Kišovce (Hozelec)	Ho 4	dump	Mn ore	TS		
54	Kišovce	Kiš 1	dump	Mn ore	TS	AES-ICP	C, REE
55	Kišovce	Kiš 2	dump	Mn ore	TS	AES-ICP	C
56	Kišovce	Kiš 3	dump	Mn ore	TS		
57	Kišovce	Kiš 10	dump	Mn ore	TS		
58	Kišovce	Kiš 11	dump	Mn ore	TS		
59	Kišovce	Kiš 12	dump	Mn ore	TS	AES-ICP	ICP,C
60	Kišovce	Kiš 13	dump	Mn ore	TS		
61	Kišovce	Kiš 14	dump	sandstone	TS		
62	Kišovce	Kiš 15	dump	Mn ore	TS	AES-ICP	C
63	Kišovce	Kiš 16	dump	Mn ore	TS	AES-ICP	C
64	Kišovce (Švábovce)	ŠV 1	dump	Mn ore	TS		
65	Kišovce (Švábovce)	Šv 2	dump	Mn ore	TS	AES-ICP	C
66	Kišovce (Švábovce)	Šv 4	dump	Mn ore	TS	AES-ICP	C
67	Kišovce (Švábovce)	Šv 5	dump	Mn ore	TS		
68	Kišovce (Švábovce)	Šv 6	dump	Mn ore	TS		
69	Kišovce (Švábovce)	Šv 7	dump	Mn ore	TS	AES-ICP	C
70	Kišovce (Švábovce)	Šv 8	dump	Mn ore	TS	AES-ICP	C
71	Kišovce (Švábovce)	Šv 9	dump	Mn ore	TS		
72	Konská	Ko-1	debris	Mn ore	TS	AES-ICP	C, REE
73	Konská	Ko-2	debris	Mn ore	TS		
74	Konská	Ko 3	debris	shale	TS		
75	Konská	Ko 4	debris	sandstone	TS		
76	Konská	Ko 5	debris	shale	TS		
77	Konská	Ko 6	debris	shale	TS		
78	Konská	Ko 7	debris	shale	TS		
79	Konská	Ko 8	debris	shale			
80	Konská, 200 m W from church road, 20 m S, path and W outcrop	Ko-9	outcrop	sandy shale	TS		
81	Konská, 200 m W from church road, 11 m S, path and W outcrop	Ko-10	outcrop	sandy shale			
82	Lednické Rovne	LR 1	dump	Mn ore	TS		
83	Lednické Rovne	LR 2	dump	Mn ore	TS	AES-ICP	C, REE
84	Lednické Rovne	LR 3	dump	Mn ore	TS2x	AES-ICP	C
85	Lednické Rovne	LR 4	dump	Mn ore	TS3x		
86	Marianka, outcrop	Ma-P-0m	outcrop	black shale, direction 134/35°		AES-ICP	C
87	Marianka, outcrop	Ma-P-1m	outcrop	black shale		AES-ICP	C
88	Marianka, outcrop	Ma-P-1.5–1.6m	outcrop	limestone	TS	AES-ICP	C
89	Marianka, outcrop	Ma-P-2m	outcrop	black shale		AES-ICP	C, REE
90	Marianka, outcrop	Ma-P-3m	outcrop	black shale		AES-ICP	C
91	Marianka, outcrop	Ma-P-3.4–3.43m	outcrop	limestone	TS	AES-ICP	C
92	Marianka, outcrop	Ma-P-4m	outcrop	black shale		AES-ICP	C
93	Marianka, outcrop	Ma-P-5m	outcrop	black shale		AES-ICP	C
94	Marianka, outcrop	Ma-P-6m	outcrop	black shale		AES-ICP	C
95	Marianka, outcrop	Ma-P-7m	outcrop	black shale		AES-ICP	C

Explanations: TS — polished thin section, V — thin section, AES-ICP — atomic emission spectroscopy with induction coupled plasma, C — rock-Eval pyrolysis for organic carbon, REE — rare earth elements analysed by atomic emission spectroscopy with induction coupled plasma.

Annexe 2: *Continued*. Part 3 from 3.

No.	Locality	No. of Sample	Source	Description	Results		
					polished thin section (TS)	AES-ICP (ICP)	C, REE
96	Marianka, outcrop	Ma-P-8 m	outcrop	black shale		AES-ICP	C
97	Marianka, outcrop	Ma-P-8.10–8.16 m	outcrop	limestone	TS	AES-ICP	C
98	Marianka, outcrop	Ma-P-9 m	outcrop	black shale		AES-ICP	C
99	Marianka, outcrop	Ma-P-9.5 m	outcrop	black shale		AES-ICP	C
100	Marianka	Ma 11	outcrop	Mn ore		AES-ICP	C
101	Marianka	Ma 12	outcrop	Mn ore		AES-ICP	C
102	Michalová	Mich 2	dump	sandstone	TS		
103	Michalová	Mich 3	dump	shale	TS		
104	Michalová	Mich 4	dump	shale	TS		
105	Michalová	Mich 5	dump	shale	TS		
106	Michalová	Mich 8	dump	Mn ore	TS	AES-ICP	C
107	Michalová	Mich 9	dump	Mn ore	TS	AES-ICP	C
108	Michalová	Mich 11	dump	Mn ore	TS	AES-ICP	C
109	Pucov	P11R1	outcrop	Mn ore	TS		C
110	Pucov	P11R2	outcrop	Mn ore	TS		C
111	Ráztočno, 150 m from northern margin of village, NE from parting of footpath, direction 60 degree, 100 m	Ra-1	outcrop	Fe-Mn oxides in shale	TS	AES-ICP	C
112	Ráztočno, 150 m from northern margin of village, NE from parting of footpath, direction 20 degree, 90 m	Ra-2	outcrop	Fe-Mn oxides in shale	TS	AES-ICP	C, REE
113	Stránske	St 1	debris	Mn ore	TS	AES-ICP	C
114	Stránske	St 2	debris	Mn ore			
115	Stránske, 20 m SW from cemetery	St-3	fragments	marl shale with Mn-Fe oxides			
116	Stránske, 20 m SW from cemetery	St-4	fragments	"			
117	Stránske, 20 m SW from cemetery	St-5	fragments	"	TS	AES-ICP	C, REE
118	Šarišské Jastrabie	ŠJ 1	outcrop	shale	N, TS	AES-ICP	C, REE
119	Šarišské Jastrabie	ŠJ-2	outcrop	Mn ore	TS		
120	Šarišské Jastrabie	ŠJ-3	outcrop	Mn ore	TS		
121	Šarišské Jastrabie	ŠJ 5	outcrop	radiolarite	TS	AES-ICP	C
122	Šarišské Jastrabie	ŠJ 6	outcrop	radiolarite	TS		
123	Šarišské Jastrabie	ŠJ 7	outcrop	radiolarite	TS		
124	Šarišské Jastrabie	ŠJ 8	outcrop	shale	TS	AES-ICP	C
125	Šarišské Jastrabie	ŠJ 9	outcrop	shale	TS	AES-ICP	C
126	Šarišské Jastrabie	ŠJ 10	outcrop	Mn ore	TS		
127	Šarišské Jastrabie	ŠJ 11	dump	Mn ore	TS		
128	Šarišské Jastrabie	ŠJ 13	outcrop	radiolarite	TS		
129	Šarišské Jastrabie	ŠJ 14	outcrop	radiolarite	TS	AES-ICP	C
130	Šarišské Jastrabie	ŠJ 15	outcrop	shale	TS	AES-ICP	C
131	Šarišské Jastrabie	ŠJ 16	outcrop	shale	TS	AES-ICP	C
132	Zázrivská dolina	Za 1	outcrop	Mn ore	TS	AES-ICP	C
133	Zázrivská dolina	Za 2	outcrop	Mn ore	TS	AES-ICP	C
134	Zázrivská dolina	Za 4	outcrop	Mn ore	TS2x		
135	Zázrivská dolina	Za 5	outcrop	shale	TS		
136	Zázrivská dolina	Za 6	outcrop	Mn ore	TS	AES-ICP	C, REE
137	Zázrivská dolina	Za 7	outcrop	Mn ore	TS	AES-ICP	C
138	Zázrivská dolina	Za 8	outcrop	shale	TS		
139	Zázrivská dolina	Za 10	outcrop	Mn ore	TS		
140	Zázrivá-Kozinská	Za 9 K	dump	Mn ore	TS	AES-ICP	C, REE
141	Zázrivská dolina	Za 3	dump	Mn ore	TS		
142	Zázrivá-Kozinská	ZaK 15	dump	shale	TS		
143	Zázrivá-Havrania	ZaH 11	dump	Mn ore	TS2x	AES-ICP	C
144	Zázrivá-Havrania	ZaH 12	dump	Mn ore	TS		
145	Zázrivá-Havrania	ZaH 13	dump	Mn ore	TS		
146	Zázrivá-Havrania	ZaH 16	dump	shale	TS		
147	Zázrivá-Havrania	ZaH 17	dump	shale	TS		
148	Zázrivá-Havrania	ZaH 18	dump	shale	TS		
149	Zázrivá-Havrania	ZaH 19	dump	Mn ore	TS	AES-ICP	C
150	Zázrivá-Havrania	ZaH 20	dump	Mn ore	TS		

Explanations: TS — polished thin section, V — thin section, AES-ICP — atomic emission spectroscopy with induction coupled plasma, C — rock-Eval pyrolysis for organic carbon, REE — rare earth elements analysed by atomic emission spectroscopy with induction coupled plasma.

Table 2a: Chemical composition of the Jurassic carbonates (WDX analyses in weight %). Part 1 from 3.

No.	Sample	CaO	MgO	FeO	MnO	SrO	BaO	CO_2	Total
1	Dik5.1	54.46	1.12	0.00	0.07	0.00	0.00	44.01	99.66
2	Dik5.2	28.18	6.51	5.96	16.65	0.03	0.02	43.23	100.59
3	Dik5.3	17.16	1.08	0.49	43.14	0.04	0.00	41.73	103.64
4	Dik5.4	17.94	1.47	0.64	39.36	0.00	0.00	40.49	99.90
5	Dik5.5	17.57	1.30	1.20	38.61	0.03	0.00	39.91	98.62
6	Dik5.6	28.96	6.96	5.88	15.74	0.00	0.01	43.69	101.24
7	dik5.7	27.74	5.80	5.43	17.14	0.04	0.01	42.08	98.24
8	Dik5.7a	27.21	5.90	5.80	19.11	0.00	0.00	43.21	101.22
9	Dik5.8	53.04	3.11	0.15	0.30	0.00	0.00	45.30	101.90
10	Dik5.11	47.32	0.78	1.12	8.76	0.14	0.00	44.17	102.29
11	Dik5.12	54.17	0.87	0.07	0.10	0.00	0.00	43.57	98.78
12	Dik5.13	48.58	0.87	1.20	8.68	0.08	0.00	45.23	104.64
13	Dik5.14	50.12	0.98	0.84	6.56	0.03	0.00	44.99	103.51
14	Dik5.15	49.61	0.63	0.81	7.08	0.11	0.00	44.56	102.80
15	Dik5.16	53.72	1.09	0.09	0.24	0.13	0.00	43.61	98.88
16	Ba1.1	18.67	1.46	1.03	38.88	0.07	0.00	41.02	101.13
17	Ba1.2	6.46	0.46	0.57	53.74	0.00	0.00	39.27	100.50
18	Ba1.3	10.41	0.76	0.80	49.49	0.04	0.00	40.21	101.71
19	Ba1.4	30.42	1.63	0.40	26.26	0.13	0.00	42.24	101.08
20	Ba1-11 t	27.81	1.38	0.55	28.80	0.14	0.00	41.60	100.28
21	Ba1-12-s	9.58	0.68	0.86	49.61	0.05	0.04	39.60	100.42
22	Ba1-13-n	9.79	1.32	4.19	45.54	0.07	0.05	39.99	100.95
23	Ba1-14-n	30.90	21.65	0.23	0.72	0.11	0.00	48.53	102.14
24	Ba1-15-n	31.93	20.61	0.23	0.68	0.00	0.00	48.13	101.58
25	Ba1-16-s	14.50	1.08	0.75	42.75	0.00	0.00	39.54	98.62
26	Ba1-17-s	24.13	1.81	1.19	30.84	0.02	0.02	40.79	98.80
27	Ba1-18 p	27.11	3.35	6.74	20.12	0.19	0.04	41.64	99.19
28	Ba1-19-t	28.40	1.54	0.87	26.75	0.04	0.00	41.11	98.71
29	Ba1-20-s	19.61	1.25	0.87	36.78	0.00	0.01	40.11	98.63
30	Ba5.1	15.43	1.11	11.06	33.64	0.05	0.00	40.99	102.28
31	Ba5.2	8.02	0.58	16.06	40.39	0.04	0.00	41.83	106.91
32	Ba5.4	53.60	0.02	0.57	0.52	0.39	0.04	42.93	98.07
33	Ba5.5	6.80	1.49	10.33	44.08	0.00	0.02	40.65	103.38
34	Ba5.6	16.02	1.26	1.57	40.83	0.08	0.00	40.28	100.04
35	Ba6.1	49.55	0.45	2.15	7.49	0.35	0.01	45.49	105.48
36	Ba6.2	46.34	0.56	2.77	9.48	0.31	0.00	44.69	104.14
37	Ba6.3	50.10	0.56	2.56	9.03	0.32	0.00	47.24	109.81
38	Ba6.4	51.81	0.38	1.80	2.66	0.76	0.00	44.15	101.56
39	BaCDD1.1	55.85	0.36	0.00	0.00	0.00	0.00	44.22	100.43
40	BaCDD1.2	55.46	0.35	0.02	0.00	0.00	0.00	43.92	99.75
41	BaCDD5-1	55.30	0.46	0.00	0.11	0.05	0.00	43.99	99.91
42	BaCDD5-2	51.70	0.28	0.12	3.11	0.02	0.00	42.89	98.12
43	BaCDD5-3	54.34	0.31	0.00	3.33	0.00	0.00	45.05	103.03
44	BaCDD5-3	54.47	0.25	0.11	1.01	0.08	0.00	43.75	99.67
45	Ba-CDH14	28.26	5.17	11.69	11.86	0.15	0.00	42.41	99.54
46	BsCD-H14	21.78	2.99	6.43	26.25	0.08	0.00	40.62	98.15
47	BaHn1-5.	28.03	1.36	1.44	27.06	0.07	0.00	41.18	99.14
48	BaHN1-5.	7.29	0.79	0.75	50.90	0.09	0.00	38.66	98.48
49	BaHN1-5.	7.68	0.86	0.73	50.12	0.04	0.00	38.52	97.95
50	BaHn1-5.	19.91	1.24	0.75	35.99	0.04	0.00	39.78	97.71
51	BaHn1-5.	7.80	0.76	0.74	50.12	0.00	0.00	38.50	97.92
52	BaHn1-6a	20.09	1.25	0.87	36.61	0.05	0.01	40.40	99.27
53	BaHn1-6a	7.57	0.95	2.24	49.53	0.07	0.03	39.12	99.51
54	BaHn1-6a	8.82	1.00	6.81	43.41	0.03	0.00	39.13	99.20
55	BaHn1-6a	26.58	2.84	7.91	19.71	0.06	0.02	41.07	98.19
56	BaHn1-6a	20.91	1.14	1.04	34.38	0.00	0.00	39.62	97.09
57	BaHn1-6a	31.85	0.36	0.09	24.90	0.00	0.00	40.89	98.09
58	BaHn1-6a	17.96	1.63	2.18	35.98	0.01	0.00	39.54	97.29
59	BaHn1-6a	26.74	1.44	0.53	28.13	0.11	0.03	40.39	97.37
60	BaHn1-6a	18.48	1.08	0.72	38.45	0.05	0.00	40.00	98.78
61	BaHn1-6a	8.53	0.87	2.54	48.26	0.05	0.03	39.17	99.45
62	BaHN1-6a	22.31	1.43	1.55	32.49	0.12	0.04	40.24	98.18
63	BaSa2-2.	24.35	1.37	0.84	30.91	0.11	0.00	40.34	97.92
64	BaSa2-2.	54.73	0.00	0.23	0.53	0.38	0.00	43.58	99.45
65	LR1	51.92	0.00	0.70	1.71	0.00	0.00	42.24	96.57
66	LR2	55.61	0.00	0.00	0.00	0.00	0.00	43.64	99.25
67	LR3	33.23	17.86	0.77	1.36	0.00	0.00	46.90	100.12
68	LR3.1	25.41	1.38	0.50	31.00	0.05	0.01	41.01	99.36
69	LR3.2	23.60	1.26	0.82	32.91	0.07	0.06	40.87	99.60
70	LR3.3	51.60	1.06	2.41	5.38	0.99	0.00	46.89	108.34

Table 2a: *Continued*. Part 2 from 3.

No.	Sample	CaO	MgO	FeO	MnO	SrO	BaO	CO_2	Total
71	LR3.4	17.49	1.77	1.89	36.57	0.08	0.01	39.55	97.36
72	LR3.5	14.09	2.19	3.65	40.03	0.01	0.01	40.53	100.51
73	LR3.6	30.64	1.87	0.76	27.09	0.08	0.04	43.41	103.91
74	LR3.7	16.27	1.69	2.12	40.30	0.14	0.02	40.99	101.54
75	LR3.8	35.78	16.17	3.33	0.30	0.05	0.00	47.98	103.60
76	LR3.9	6.94	9.80	24.62	15.64	0.04	0.16	40.99	98.18
77	LR3.10	7.00	7.43	20.49	20.10	0.05	0.06	38.66	93.79
78	LR3.11	52.99	0.66	2.07	5.58	0.32	0.01	47.18	108.81
79	LR3.12	14.96	1.51	2.24	39.25	0.05	0.06	39.15	97.21
80	LR3.13	54.99	0.28	1.12	3.87	0.20	0.00	46.64	107.10
81	LR3.14	20.62	1.16	0.58	37.10	0.06	0.06	40.86	100.44
82	Za1zilka	50.05	0.40	0.96	5.37	0.00	0.00	43.63	100.41
83	Za1tmelt	48.99	0.54	0.40	5.74	0.00	0.00	42.84	98.51
84	Za 1 sve	31.29	4.66	5.41	12.59	0.00	0.00	40.77	94.72
85	Za1 svet	31.45	4.36	5.31	13.14	0.00	0.00	40.85	95.11
86	Za2.1	8.51	7.89	13.66	27.41	0.00	0.11	40.70	98.29
87	Za2.2	18.30	1.08	0.32	40.00	0.00	0.01	40.56	100.27
88	Za2.3	19.14	1.14	0.31	39.51	0.02	0.03	40.99	101.16
89	Za2.4	30.17	15.84	3.95	4.58	0.18	0.34	46.40	101.45
90	Za2.5	50.44	0.86	0.81	9.77	0.08	0.00	47.12	109.09
91	Za2.6	29.35	15.37	4.63	4.73	0.15	0.25	45.73	100.21
92	Za2.7	17.14	1.39	1.44	41.78	0.11	0.04	41.84	103.74
93	Za2.8	23.04	1.03	0.40	34.60	0.09	0.03	40.97	100.18
94	Za2.9	20.92	1.38	0.84	35.99	0.05	0.02	40.78	99.97
95	Za2.10	11.47	1.54	2.20	46.82	0.08	0.07	41.14	103.32
96	ZA5.1	47.25	0.77	0.65	7.37	0.11	0.00	42.94	99.09
97	Za5.2sv	31.42	4.03	5.36	16.34	0.02	0.00	42.49	99.66
98	Za5.3 tm	46.57	0.92	0.88	7.59	0.13	0.00	42.85	98.94
99	Za5.4 sv	19.30	1.05	0.37	38.35	0.00	0.04	40.32	99.43
100	Za5.5 sv	16.03	1.23	0.50	40.81	0.00	0.00	39.55	98.12
101	Za5.6 tm	18.34	1.34	0.55	38.13	0.00	0.01	39.85	98.22
102	Za5.7 sv	17.39	0.95	0.33	39.76	0.07	0.05	39.60	98.15
103	Za6 kt	23.10	1.79	0.81	30.18	0.00	0.00	39.30	95.18
104	Za6kt	19.77	1.20	0.56	36.42	0.04	0.00	39.78	97.77
105	Za6kt	23.32	1.62	1.00	30.17	0.06	0.00	39.43	95.60
106	Za6ka	52.48	1.41	0.35	3.04	0.19	0.00	44.91	102.38
107	Za6ka	46.53	0.69	0.71	10.35	0.25	0.00	44.23	102.76
108	Za6ka	49.89	0.49	0.81	5.53	0.24	0.00	43.72	100.68
109	Za6ka	51.44	0.82	0.73	8.82	0.00	0.00	47.18	108.99
110	ZaK9.1	19.74	2.16	0.38	34.19	0.05	0.00	39.32	95.84
111	Za11.1	59.42	0.78	0.60	1.29	0.10	0.00	48.69	110.88
112	Za12.1 s	8.73	3.02	10.67	35.71	0.06	0.04	38.88	97.11
113	Za12.2 t	26.77	1.44	1.07	28.14	0.06	0.00	40.72	98.20
114	Za12.3 n	32.08	18.89	0.39	3.76	0.51	0.00	48.59	104.22
115	Za12.4 n	48.23	1.36	3.56	4.85	0.60	0.00	44.78	103.38
116	Za12.5 n	30.35	18.57	0.73	3.55	0.04	0.00	46.76	100.00
117	Za12.6 s	10.11	4.09	13.67	30.81	0.00	0.07	39.91	98.66
118	Za12.7 s	54.28	0.12	0.87	0.53	0.10	0.00	43.63	99.53
119	Za12.8 s	11.85	1.41	1.96	43.99	0.02	0.01	39.34	98.58
120	Za12.9 s	9.42	5.20	19.27	24.76	0.03	0.09	40.27	99.04
121	Za12.10	28.63	1.68	1.56	25.75	0.11	0.00	41.28	99.01
122	Za15.1	52.43	0.49	0.95	3.30	0.03	0.00	44.32	101.52
123	Za15.2	54.21	0.68	0.25	0.91	0.06	0.00	44.03	100.14
124	Za17.1 t	51.60	3.41	0.09	0.06	0.20	0.00	44.40	99.76
125	Za17.2 s	49.10	0.60	1.30	4.21	0.00	0.00	42.60	97.81
126	Za17.3 s	51.66	0.71	0.69	2.54	0.36	0.00	43.47	99.43
127	Za17.4 t	55.61	0.28	0.00	0.05	0.03	0.02	44.00	99.99
128	Za17.5 t	54.77	0.01	0.18	0.16	0.15	0.00	43.27	98.54
129	Za17.6 s	14.77	0.97	0.22	43.87	0.01	0.03	40.02	99.89
130	Za17.7 s	11.79	1.72	0.69	44.14	0.12	0.00	38.99	97.45
131	Za17.8 s	14.18	0.88	0.33	44.57	0.00	0.00	39.94	99.90
132	Za17.9 s	22.78	1.33	0.36	31.99	0.06	0.12	39.46	96.10
133	Za17.10	21.09	1.31	0.32	34.60	0.07	0.11	39.70	97.20
134	Za17.11	54.03	0.02	0.30	0.04	0.27	0.00	42.75	97.41
135	Za17.12	27.80	1.86	0.37	28.51	0.10	0.00	41.80	100.44
136	ZaH19svf	5.09	6.88	27.46	17.19	0.00	0.00	38.99	95.61
137	ZaH19tm	29.95	1.48	0.64	25.76	0.21	0.00	41.58	99.62
138	ZaH19tm	32.01	1.32	0.83	22.29	0.06	0.00	40.92	97.43
139	ZaH19tm	28.59	1.33	1.38	25.88	0.13	0.00	40.85	98.16
140	ZaH19tm	28.14	1.73	1.39	25.62	0.09	0.00	40.76	97.73

Table 2a: *Continued*. Part 3 from 3.

No.	Sample	CaO	MgO	FeO	MnO	SrO	BaO	CO_2	Total
141	ZaH19pre	23.74	1.28	0.66	31.11	0.15	0.00	39.80	96.74
142	ZaH19sv	24.60	1.35	0.39	30.51	0.00	0.00	39.95	96.80
143	SJ2	3.52	1.89	20.90	33.34	0.00	0.00	38.31	97.96
144	SJ2	3.52	1.89	20.90	34.34	0.00	0.00	38.93	99.58
145	SJ9-19	0.55	2.01	32.79	23.42	0.00	0.00	37.24	96.01
146	SJ9-18	4.31	1.99	21.18	30.62	0.00	0.00	37.52	95.61
147	SJ16-11	2.15	2.04	28.48	24.57	0.00	0.00	36.61	93.86
148	SJ9	3.23	1.97	22.83	31.62	0.00	0.00	38.29	97.94
169	SJ10.1	4.63	2.04	23.05	30.95	0.01	0.00	39.19	99.87
150	SJ10.2	3.50	1.97	22.43	33.00	0.01	0.00	39.12	100.03
151	SJ16.1	10.20	1.93	2.16	43.13	0.01	0.00	38.20	95.63
152	SJ16.2	3.09	2.04	30.54	26.51	0.00	0.00	39.81	101.99
153	SJ16.3	6.67	2.00	13.12	37.75	0.02	0.00	38.88	98.44
154	SJ16.4	2.36	2.13	32.77	25.19	0.00	0.00	39.88	102.33
155	MaP1.5.1	51.68	0.53	0.78	0.28	2.51	0.00	42.85	98.63
156	MaP1.5.2	53.64	0.37	1.05	0.34	0.20	0.00	43.43	99.02
157	MaP1.5.3	53.69	0.34	1.14	0.34	0.09	0.00	43.45	99.05
158	MaP1.5.4	53.34	0.43	0.61	0.24	1.57	0.00	43.51	99.69
159	MaP1.5.5	53.90	0.26	0.96	0.47	0.14	0.00	43.52	99.24
160	MaP1.5.6	53.21	0.47	0.73	0.37	1.78	0.00	43.70	100.26
161	MaP1.5.7	53.21	0.42	0.65	0.17	1.83	0.00	43.51	99.80
162	MaP7b.8s	55.98	0.07	0.28	0.18	0.03	0.00	44.30	100.83
163	MaP7b.9s	53.14	1.51	0.16	0.00	0.03	0.00	43.47	98.31
164	MaP7b.10	54.14	0.54	0.61	0.13	0.17	0.00	43.60	99.19

	CaO	MgO	FeO	MnO	SrO	BaO	CO_2	Total
Average	29.86	2.40	3.92	21.64	0.13	0.01	41.94	99.90
minimum	0.55	0.00	0.00	0.00	0.00	0.00	36.61	
maximum	59.42	21.65	32.79	53.74	2.51	0.34	48.69	
n	164	164	164	164	164	164	164	

Table 2b: Chemical composition of the Paleogene carbonates (WDX analyses in weight %). Part 1 from 2.

No.	Sample	CaO	MgO	FeO	MnO	SrO	BaO	CO_2	Total
1	Ra2a.3	56.40	0.13	0.01	0.04	0.00	0.00	44.44	101.03
2	Ra1.2	56.00	0.33	0.02	0.01	0.00	0.00	44.32	100.68
3	Ho3.3 sv	13.11	1.27	0.31	44.98	0.00	0.00	39.77	99.44
4	Ho3.5 sv	11.40	1.81	0.98	43.83	0.00	0.00	38.72	96.74
5	Ho3.8 tm	30.54	22.10	0.13	0.63	0.00	0.00	48.57	101.97
6	MnKis1/1	29.47	2.16	0.00	23.38	0.00	0.00	39.99	95.00
7	MnKis1/3	25.64	1.71	0.00	28.42	0.00	0.00	39.62	95.39
8	MnKis1/5	24.54	1.96	0.59	29.97	0.00	0.00	40.35	97.41
9	Sv7sv	10.97	1.09	0.57	45.06	0.00	0.00	38.10	95.79
10	Sv8.2 sv	6.41	0.99	0.65	51.88	0.00	0.05	38.71	98.69
11	Sv8.5 tm	30.50	20.45	0.18	1.17	0.00	0.00	47.10	99.40
12	Sv8.6 st	31.73	1.83	0.19	22.46	0.00	0.10	40.98	97.29
13	Sv8.7 tm	30.58	21.49	0.12	0.37	0.00	0.02	47.77	100.35
14	Sv8.9 sv	9.04	1.73	0.83	46.53	0.00	0.00	38.36	96.49
15	Ko2-klas	31.76	20.28	0.00	0.00	0.00	0.00	47.07	99.11
16	Ko2-karb	48.04	0.48	3.24	3.15	0.00	0.00	42.16	97.07
17	Ko3-1	54.14	0.82	0.07	0.03	0.00	0.00	43.44	98.50
18	Ko3-2	53.96	0.38	1.37	0.62	0.00	0.00	43.99	100.32
19	Mich11bt	45.14	1.95	2.45	8.18	0.00	0.00	44.13	101.85
20	Mich11bs	6.58	1.14	1.47	48.73	0.00	0.00	37.54	95.46
21	Mich11b	46.77	1.69	2.02	8.05	0.00	0.00	44.78	103.31
22	Mich11b	46.30	1.97	2.20	8.35	0.00	0.00	45.01	103.83
23	ByP9.5b	55.95	0.35	0.33	0.09	0.00	0.00	44.55	101.26
24	ByP9.5b	55.65	0.33	0.14	0.03	0.00	0.00	44.14	100.29
25	P11R1	16.02	1.61	2.31	38.44	0.00	0.00	39.59	97.96
26	P11R1	21.14	1.62	2.47	33.18	0.00	0.00	40.46	98.87
27	ByP9.5c	55.20	0.41	0.16	0.05	0.00	0.00	43.89	99.70
28	ByP5.7	56.12	0.24	0.10	0.06	0.01	0.00	44.41	100.93
29	Ho3.6 sv	11.87	1.52	1.03	44.92	0.02	0.01	39.49	98.86
30	Kis2-105	11.38	1.84	1.07	43.46	0.02	0.01	38.57	96.35
31	Kis10.9	20.08	1.66	0.36	35.58	0.02	0.00	39.87	97.57
32	P11R1	18.52	2.13	5.02	32.07	0.02	0.01	39.84	97.61
33	ByP9.5c	50.58	0.63	1.24	2.01	0.03	0.01	42.40	96.89
34	ByP5.5a	53.65	0.71	0.71	0.11	0.03	0.00	43.40	98.61
35	Ra2a.2	54.25	0.78	0.95	0.12	0.03	0.00	44.10	100.23
36	Kis2-105	14.38	1.66	0.41	41.10	0.03	0.03	38.87	96.48
37	Sv8.10 s	15.49	1.54	0.64	40.32	0.03	0.00	39.26	97.28
38	Sv8.11 s	5.68	0.96	0.53	53.68	0.03	0.02	39.15	100.05
39	Ko3-3	54.36	0.38	1.27	0.70	0.03	0.00	44.30	101.04
40	By3	55.55	0.46	0.78	0.11	0.03	0.00	44.66	101.59
41	By3	44.76	0.72	3.85	2.02	0.03	0.02	39.54	90.94
42	P11R1	19.49	1.81	4.99	32.61	0.03	0.01	40.58	99.52
43	ByP5.1	8.87	0.56	1.44	49.67	0.03	0.11	39.31	100.00
44	Ra2a.4	54.19	0.17	0.22	0.08	0.04	0.01	42.91	97.62
45	Sv8.8sv	9.21	1.31	0.40	48.56	0.04	0.00	39.05	98.57
46	Mich11bs	6.07	1.71	3.04	46.55	0.04	0.00	37.39	94.80
47	Ra2a.5	54.21	0.73	0.48	0.51	0.05	0.00	43.96	99.93
48	Ho1tm	43.49	2.07	2.40	10.44	0.05	0.00	44.36	102.81
49	Kis2-105	41.63	1.56	1.80	10.36	0.05	0.00	41.93	97.33
50	Sv7tm	42.66	2.82	1.88	10.76	0.05	0.00	44.41	102.58
51	Mich11b	6.24	1.16	1.65	48.97	0.05	0.00	37.58	95.65
52	By3	55.24	0.75	0.06	0.02	0.05	0.00	44.24	100.36
53	Ra1.1	54.88	0.84	0.10	0.09	0.06	0.00	44.13	100.11
54	Ho3.7 st	29.29	2.17	0.13	25.50	0.07	0.00	41.29	98.45
55	Kis10.2	40.06	2.65	2.46	11.15	0.07	0.00	42.79	99.18
56	P11R1	25.74	1.44	3.00	28.42	0.07	0.00	41.27	99.94
57	Ho3.4 st	26.23	1.67	0.32	29.74	0.08	0.00	41.09	99.13
58	Kis2-105	40.49	1.78	2.14	9.55	0.08	0.02	40.99	95.05
59	Kis10.8	19.56	1.93	0.37	35.27	0.08	0.00	39.60	96.81
60	P11R1	47.92	1.74	3.82	5.27	0.08	0.02	45.16	104.01
61	Ho3.1 tm	44.55	1.31	1.48	7.12	0.09	0.00	41.75	96.30
62	Kis2-105	26.51	2.03	0.11	27.53	0.09	0.00	40.21	96.48
63	Kis10.5	38.91	1.92	0.12	14.26	0.09	0.00	41.59	96.89
64	Sv8.12 s	6.79	0.57	0.48	54.59	0.09	0.02	40.16	102.70
65	Ra1.3	54.47	0.88	0.20	0.09	0.09	0.00	43.93	99.66
66	Sv7tm	32.55	1.65	0.14	23.20	0.10	0.00	41.87	99.51
67	Sv8.3 st	26.58	1.68	0.31	28.60	0.10	0.00	40.67	97.94
68	ByP5.5	53.35	1.25	0.42	0.29	0.11	0.00	43.72	99.14
69	Kis2-120	52.73	0.26	0.30	0.00	0.11	0.00	41.90	95.30
70	Kis10.1	39.59	2.75	2.47	11.17	0.11	0.00	42.56	98.65

Table 2b: *Continued*. Part 2 from 2.

No.	Sample	CaO	MgO	FeO	MnO	SrO	BaO	CO_2	Total
71	Sv8.4 tm	30.72	21.08	0.08	2.27	0.11	0.00	48.63	102.89
72	Ra2a.1	49.76	0.23	4.88	0.41	0.12	0.00	42.59	97.99
73	Kis10.3	50.47	2.04	1.17	4.91	0.12	0.00	45.65	104.36
74	Mich4-1	47.28	0.14	6.46	0.58	0.12	0.00	41.63	96.21
75	By3	52.03	0.37	0.87	2.75	0.12	0.00	43.53	99.67
76	Sv7tm	15.33	2.34	0.79	37.59	0.13	0.00	38.45	94.63
77	Sv8.1 st	32.49	2.02	0.17	21.72	0.13	0.00	41.34	97.87
78	Ho1sv	13.72	1.53	0.52	42.18	0.14	0.00	38.98	97.07
79	Ho3.9 st	30.59	2.17	0.19	23.45	0.14	0.00	41.10	97.64
80	Michh11b	49.19	1.40	1.91	8.21	0.14	0.00	46.45	107.30
81	By3	51.92	0.36	1.03	2.88	0.14	0.00	43.62	99.95
82	ByP5.4	54.40	0.15	0.47	0.45	0.15	0.02	43.49	99.12
83	Kis2-105	9.86	1.22	0.24	46.31	0.15	0.01	38.01	95.80
84	By1c	54.58	1.02	0.12	0.00	0.15	0.00	44.08	99.95
85	Kis10.4	48.23	1.61	1.05	4.37	0.16	0.00	43.03	98.45
86	Kis10.10	20.96	1.56	0.41	38.06	0.16	0.00	42.08	103.23
87	Sv7tm	35.53	2.10	0.09	18.85	0.16	0.00	41.99	98.72
88	Ho3.2 tm	45.98	1.43	1.87	7.25	0.17	0.00	43.36	100.06
89	Sv7sv	10.85	0.98	0.56	47.45	0.18	0.00	39.44	99.46
90	Mich4-2	54.10	0.35	0.88	0.32	0.18	0.01	43.66	99.50
91	Ho1tm	43.30	2.34	2.83	11.28	0.20	0.00	45.35	105.30
92	Kis10.7	38.82	1.73	0.16	14.57	0.21	0.03	41.59	97.11
93	Ho1sv	12.72	1.84	1.27	40.85	0.22	0.00	38.21	95.11
94	Kis10.6	39.04	1.82	0.12	13.66	0.24	0.00	41.28	96.16
95	ByP9.5c	50.92	0.54	1.70	3.12	0.24	0.02	43.63	100.17
96	Kis2-105	54.70	0.11	0.12	0.46	0.25	0.01	43.52	99.17
97	ByP9.5c	51.47	1.28	0.58	2.57	0.25	0.00	43.85	100.00
98	P11R1	50.99	0.41	1.28	3.43	0.29	0.00	43.50	99.90
99	Ho1tm	41.73	2.20	2.51	10.83	0.31	0.00	43.54	101.12
100	ByP5.9	50.58	0.26	0.70	3.32	0.33	0.06	42.63	97.88
101	ByP5.11	51.58	0.38	1.08	1.94	0.56	0.00	42.99	98.53
102	ByP5.6	51.47	0.40	0.94	2.35	0.56	0.00	43.10	98.82
103	ByP5.10	51.47	0.36	1.08	2.58	0.59	0.00	43.30	99.38
104	ByP5.8	51.20	0.41	1.03	2.37	0.70	0.00	43.01	98.71
		3769.12	228.63	116.65	1777.61	10.21	0.63	4386.38	
		CaO	**MgO**	**FeO**	**MnO**	**SrO**	**BaO**	**CO_2**	**Total**
	Average	36.24	2.20	1.12	17.09	0.098	0.006	42.17	98.92
	minimum	5.68	0.11	0.00	0.00	0.00	0.00	37.39	
	maximum	56.40	22.10	6.46	54.59	0.70	0.11	48.63	
	n	104							

Table 3a: Chemical composition of rancieite (weight %). Part 1 from 2.

No.	Sample	MnO_2	CaO	Fe_2O_3	MgO	SiO_2	K_2O	BaO	Al_2O_3	SrO	P_2O_5	Na_2O	Total
1	Dik7.3	83.60	4.39	0.75	1.32	0.07	0.27	0.01	0.51	0.17	0.00	0.13	91.22
2	Dik7.5	81.40	4.28	3.49	1.23	0.13	0.21	0.00	0.34	0.05	0.04	0.19	91.35
3	Dik7.6	85.02	4.64	0.52	1.26	0.02	0.23	0.00	0.19	0.06	0.04	0.18	92.16
4	Dik7.7	84.56	4.68	0.88	1.24	0.06	0.25	0.00	0.13	0.08	0.00	0.22	92.10
5	Dik7.8	83.66	4.61	1.12	1.25	0.26	0.24	0.00	0.22	0.07	0.00	0.17	91.59
6	Dik6b.1	82.29	4.33	1.20	1.86	0.03	0.47	0.00	0.18	0.00	0.01	0.20	90.57
7	Dik6b.2	83.37	2.68	0.80	3.16	0.29	0.50	0.03	0.24	0.05	0.03	0.33	91.48
8	Dik6b.3	83.60	6.82	1.04	1.47	1.23	0.38	0.00	0.67	0.01	0.02	0.03	95.28
9	Dik6b.4	83.15	7.17	1.47	1.44	0.59	0.21	0.00	0.35	0.06	0.04	0.01	94.50
10	Dik6b.5	79.98	6.25	0.63	1.36	3.36	0.25	0.01	1.28	0.00	0.02	0.02	93.16
11	Dik5.10	82.91	4.21	0.33	1.70	0.06	0.67	0.19	0.18	0.25	0.00	0.22	90.72
12	Ba-6b ana1 sv	82.05	5.26	0.66	1.37	0.02	0.19	0.01	0.02			0.00	89.58
13	Ba-6b ana3	81.20	5.04	1.24	1.23	0.03	0.18	0.00	0.06			0.00	88.98
14	Ba-6b ana4	82.48	5.20	0.65	1.20	0.01	0.17	0.00	0.02			0.00	89.73
15	Ba-6b ana5	84.26	5.31	0.61	1.10	0.03	0.19	0.00	0.01			0.00	91.51
16	Ba-6b ana6	83.96	5.15	0.61	1.11	0.00	0.17	0.00	0.02			0.00	91.02
17	Ba-6b ana7	74.23	4.72	8.39	1.01	0.37	0.14	0.02	0.25			0.00	89.13
18	CD-D7 an1	77.07	7.57	0.45	0.78	0.10	0.52	0.09	0.05			0.00	86.63
19	CD-D7 an2	77.35	7.74	0.40	0.69	0.23	0.54	0.01	0.04			0.00	87.00
20	CD-D7 an3	77.67	7.12	0.57	0.83	0.23	0.48	0.13	0.03			0.00	87.06
21	CD-D7 an4	78.15	7.67	0.46	0.72	0.08	0.51	0.07	0.05			0.00	87.71
22	CD-D7 an5	80.80	6.96	0.42	0.94	0.08	0.76	0.07	0.00			0.00	90.03
23	CD-D7 an6	79.26	7.01	0.55	1.01	0.36	0.64	0.14	0.06			0.00	89.03
24	CD-D7 an7	79.95	6.93	0.41	1.02	0.67	0.49	0.15	0.43			0.00	90.05
25	CD-D7 an8	76.24	8.57	2.16	0.51	0.27	0.52	0.03	0.10			0.00	88.40
26	CD-D7 an9	72.93	6.30	5.94	0.99	0.63	0.53	0.08	0.24			0.00	87.64
27	CD-D7 an10	78.42	7.55	0.60	0.79	0.15	0.53	0.08	0.06			0.00	88.18
28	CD-D7 an11	80.29	5.24	0.83	1.31	0.17	1.02	0.22	0.00			5.00	94.08
29	CD-D7 an12	81.01	5.15	0.82	1.40	0.12	1.13	0.15	0.00			0.00	89.78
30	CD-D7 an13	80.52	5.62	1.01	1.27	0.15	0.99	0.19	0.08			0.00	89.83
31	CD-D7 an14	78.02	8.42	0.83	0.60	0.16	0.67	0.02	0.04			0.00	88.76
32	CD-D7 an15	78.50	8.24	0.95	0.59	0.11	0.46	0.05	0.02			0.00	88.92
33	CD-D7 an16	72.38	5.96	8.45	1.00	1.01	0.45	0.09	0.28			0.00	89.62
34	CD-D7 an17	80.33	4.78	3.64	1.44	0.30	0.98	0.03	0.03			0.00	91.53
35	CD-D7 an18	81.68	4.39	0.98	1.61	0.14	1.08	0.07	0.02			0.00	89.97
36	CD-D7 an19	79.79	4.71	2.18	1.50	0.29	1.05	0.08	0.03			0.00	89.63
37	CD-H1 an1	83.80	3.32	0.65	0.90	0.10	0.60	0.00	0.41			0.00	89.78
38	CD-H1 an2	88.50	3.23	0.20	0.63	0.06	0.53	0.00	0.04			0.00	93.19
39	CD-H1 an3	84.19	3.63	0.49	0.97	0.04	0.46	0.01	0.17			0.00	89.96
40	CD-H1 an4	85.18	3.55	0.62	0.93	0.06	0.57	0.00	0.55			0.00	91.46
41	CD-H1 an5	86.72	3.62	0.22	0.57	0.06	0.57	0.00	0.03			0.00	91.79
42	CD-H1 an6	85.69	3.28	0.25	0.72	0.06	0.63	0.00	0.35			0.00	90.98
43	CD-H1 an7	80.26	3.18	3.92	0.87	0.27	0.58	0.00	0.82			0.00	89.90
44	CD-H1 an8	83.39	3.27	0.59	1.15	0.06	0.74	0.00	0.16			0.00	89.36
45	CD-H1 an9	82.61	3.63	1.22	0.97	0.37	0.71	0.00	0.47			0.00	89.98
46	ČD-H1	84.98	3.58	0.42	0.00	0.02	0.53	0.00	0.34			0.00	89.87
47	ČD-H1	85.31	3.54	0.38	0.00	0.00	0.56	0.04	0.09			0.00	89.92
48	ČD-D7	80.56	4.73	3.14	0.00	0.18	0.90	0.07	0.07			0.00	89.65
49	ČD-D7	77.68	7.74	0.56	0.00	0.02	0.48	0.07	0.07			0.00	86.62
50	CDD7.1	78.08	7.60	0.44	0.80	0.11	0.55	0.08	0.06			0.03	87.75
51	CDD7.2	75.80	7.53	0.69	0.81	0.17	0.51	0.08	0.08			0.03	85.70
52	CDD7.3	78.70	7.26	0.41	0.93	0.09	0.76	0.06	0.06			0.05	88.32
53	CDD7.4	74.11	8.42	2.75	0.56	0.39	0.46	0.04	0.13			0.07	86.93
54	CDD7.5	76.70	8.76	0.76	0.51	0.17	0.45	0.02	0.06			0.11	87.54
55	CDD7.6	75.96	8.68	0.46	0.46	0.24	0.45	0.00	0.09			0.04	86.38
56	CDD7.7	78.14	9.18	0.92	0.48	0.15	0.46	0.02	0.26			0.04	89.65
57	CDD7.8	71.76	9.58	2.06	0.40	0.28	0.42	0.00	0.30			0.11	84.91
58	CDH1.2	79.88	3.62	2.56	0.86	0.24	0.43	0.00	0.85			0.11	88.55
59	CDH1.3	81.99	3.13	2.77	0.98	0.15	0.71	0.00	0.25			0.39	90.37
60	CDH1.4	79.41	3.41	3.92	0.91	0.34	0.48	0.06	0.76			0.38	89.67
61	CDH1.5	84.55	3.36	0.43	0.71	0.09	0.66	0.00	0.38			0.70	90.88
62	CDH1.6	85.31	3.54	0.93	0.56	0.02	0.54	0.00	0.09			0.94	91.93
63	CDH1.7	84.01	3.57	0.47	0.83	0.09	0.59	0.00	0.45			0.71	90.72
64	LR2.1	80.02	8.40	0.00	0.00	0.18	0.35	0.00	0.00			0.00	88.95
65	LR2.1svf	81.08	6.39	1.91	0.00	0.33	0.55	0.30	0.00			0.00	90.56
66	LR2.3	80.53	10.10	0.00	0.00	0.00	0.23	0.00	0.00			0.00	90.86
67	LR2.4	78.56	6.00	1.88	0.00	0.20	0.58	0.00	0.00			0.00	87.22
68	LR1	81.02	5.03	0.89	0.43	0.20	0.94	0.13	0.00			0.00	88.64
69	By1a	80.23	5.93	0.87	0.88	0.02	0.53	0.00	0.01	0.21		0.16	88.85
70	By1a	79.36	6.00	0.53	0.81	0.04	0.47	0.00	0.00	0.21		0.15	87.58

Table 3a: *Continued*. Part 2 from 2.

No.	Sample	MnO_2	CaO	Fe_2O_3	MgO	SiO_2	K_2O	BaO	Al_2O_3	SrO	P_2O_5	Na_2O	Total
71	By1a	80.74	6.39	0.31	0.71	0.00	0.46	0.00	0.00	0.14		0.12	88.88
72	By1a	81.01	7.21	0.81	0.65	0.00	0.40	0.00	0.02	0.19		0.11	90.39
73	By1a	78.96	10.14	1.04	0.27	0.02	0.20	0.00	0.32	0.01		0.07	91.04
74	By1c	80.50	8.86	0.29	0.36	0.02	0.18	0.06	0.06	0.11		0.04	90.47
75	By1c	79.44	8.90	0.74	0.23	0.04	0.11	0.04	0.13	0.02		0.03	89.69
76	By1c	79.23	9.16	0.51	0.33	0.04	0.16	0.00	0.11	0.00		0.05	89.61
77	By2a	69.42	4.94	11.14	1.00	0.49	0.61	0.25	0.26	0.08		0.08	88.27
78	By2a	81.15	5.96	1.02	1.03	0.02	0.77	0.35	0.02	0.04		0.09	90.44
79	By2a	82.49	5.93	1.26	1.04	0.00	0.73	0.36	0.02	0.07		0.15	92.06
80	By2b	67.00	5.51	11.21	0.50	0.75	0.33	0.06	0.23	0.26		0.04	85.88
81	By2b	78.33	5.50	5.55	1.03	0.30	0.00	0.06	0.19	0.18		0.07	91.19
82	By2b	78.57	5.86	6.82	0.93	0.30	0.47	0.01	0.21	0.30		0.04	93.50
83	ByP9.5b	80.92	5.50	0.60	1.06	0.04	0.72	0.11	0.00	0.26	0.00	0.12	89.33
84	ByP9.5b	80.80	5.49	0.34	1.16	0.02	0.75	0.10	0.00	0.30	0.00	0.10	89.08
85	ByP9.5b	79.12	5.95	0.45	0.96	0.01	0.66	0.12	0.01	0.24	0.01	0.09	87.61
86	ByP9.5b	81.50	5.18	0.52	1.18	0.01	0.76	0.12	0.01	0.30	0.01	0.11	89.69
87	ByP9.5b	81.01	5.87	1.13	0.98	0.02	0.50	0.01	0.00	0.22	0.00	0.10	89.85
88	ByP9.5b	64.89	7.21	13.13	0.45	0.49	0.17	0.01	0.59	0.17	0.59	0.06	87.18
89	ByP9.5b	70.51	7.41	6.62	0.53	0.24	0.26	0.01	0.25	0.16	0.25	0.07	86.07
90	ByP9.5b	78.95	7.46	0.36	0.72	0.04	0.40	0.02	0.04	0.20	0.04	0.10	88.29
91	ByP9.5a	80.22	7.81	0.36	0.67	0.03	0.42	0.02	0.05	0.18	0.05	0.13	89.90
92	ByP11a.2	81.15	5.98	0.54	0.91	0.24	0.60	0.24	0.09	0.16	0.09	0.17	90.13
93	ByP11a.2	79.16	5.77	0.64	0.87	0.15	0.60	0.26	0.19	0.18	0.19	0.15	88.01
94	ByP11a.2	79.43	7.01	0.43	0.61	0.00	0.50	0.15	0.07	0.23	0.07	0.10	88.53
95	ByP11a.2	79.51	7.27	0.32	0.57	0.01	0.47	0.02	0.02	0.18	0.02	0.18	88.57
96	ByP11a.3	80.62	5.99	0.51	0.85	0.04	0.63	0.10	0.05	0.28	0.05	0.17	89.25
97	ByP9c.31	75.69	8.08	0.48	0.61	2.05	0.49	0.10	1.83	0.09	1.83	0.05	89.48
98	ByP9.5c	73.87	7.76	0.47	0.75	1.39	0.32	0.05	0.96	0.12	0.96	0.07	85.78
99	ByP9.5c	78.91	8.19	0.61	0.46	0.01	0.17	0.01	0.12	0.06	0.12	0.01	88.56
100	ByP5.2	72.37	10.57	0.98	0.61	0.89	0.13	0.11	2.29	0.06	2.29	0.00	88.02
101	St5.2	84.80	7.64	1.03	0.54	0.24	0.40	0.03	0.19	0.07	0.05	0.06	95.05
102	St5.3	78.62	8.61	1.30	0.35	0.32	0.15	0.00	0.13	0.21	0.29	0.06	90.03
103	St5.4	76.44	8.76	2.65	0.42	1.15	0.19	0.05	0.59	0.13	0.29	0.04	90.71
104	St5.5	80.42	9.86	0.76	0.61	1.51	0.31	0.03	0.83	0.10	0.05	0.13	94.62
105	Ra2b.1	76.59	10.72	0.75	0.12	0.10	0.18	0.06	0.27	0.03	0.03	0.09	88.95
106	Ra2b.2	77.77	10.59	0.60	0.13	0.06	0.20	0.06	0.22	0.02	0.04	0.04	89.73
107	Ra2b.3	78.55	9.48	0.80	0.15	0.04	0.08	0.38	0.01	0.09	0.01	0.08	89.66
108	Ra2b.4	81.67	11.18	0.55	0.10	0.10	0.07	0.05	0.20	0.01	0.01	0.05	94.05
109	Ra2b.5	73.32	9.20	6.67	0.22	0.49	0.09	0.59	0.54	0.05	0.20	0.08	91.44
110	Ra2b.6	75.69	11.40	1.44	0.15	0.21	0.27	0.49	0.21	0.07	0.22	0.04	90.02
111	Kis16–12	79.72	9.35	0.55	0.45	0.75	0.31	0.02					91.11
112	Kis16–12	78.49	9.18	0.46	0.51	0.98	0.69	0.00					89.93
113	Kis16–12	70.61	5.90	4.22	1.16	4.09	0.62	0.08					86.75
114	Kis16–12	82.28	5.55	0.65	1.40	0.06	0.74	0.03					90.59
115	Kis16–12	82.49	5.89	0.28	1.40	0.59	0.58	0.00					91.39
116	kis16–12	82.03	6.42	0.34	1.16	0.02	1.10	0.00					90.55
117	Mich9b-1	88.35	1.29	0.47	0.21	0.43	0.48	0.00					91.85
118	Mich9b-1	89.45	1.99	0.89	0.25	0.26	0.44	0.05					93.37
119	Mich9b-1	90.32	1.77	2.19	0.23	0.43	0.41	0.07					95.45
120	Mich9b-1	90.31	1.17	0.80	0.37	0.85	0.55	0.05					93.96
121	Mich9b-1	77.99	8.17	0.90	0.62	0.59	0.44	0.00					88.82
123	Mich9b-1	77.57	8.23	0.59	0.62	0.67	0.33	0.03					88.15
124	Mich9b-1	80.17	8.71	0.45	0.71	0.20	0.49	0.02					90.59
125	Mich9b-1	77.60	8.67	0.60	0.63	0.50	0.17	0.02					88.51
126	Mich9a-1	80.44	9.09	0.37	0.62	0.00	0.40	0.00					90.69
127	Ko1-106	83.74	6.31	0.47	0.53	0.08	0.36	0.00					91.53
128	Ko1-106	83.01	6.21	0.47	0.53	0.65	0.38	0.06					91.29
129	Ko1-124	82.76	4.37	0.24	0.89	0.02	0.38	0.01					88.67

Table 3b: Chemical composition of pyrolusite (weight %).

No.	Sample	MnO_2	Fe_2O_3	SiO_2	Al_2O_3	MgO	CaO	BaO	K_2O	Total
1	Ba-1	98.04	0.18	0.28	0.00	0.02	0.14	0.00	0.02	98.69
2	Ba-1	98.88	0.18	0.17	0.02	0.02	0.27	0.00	0.01	99.55
3	Ba-1	99.70	0.20	0.14	0.00	0.01	0.17	0.00	0.00	100.23
4	Ba-1	100.07	0.19	0.09	0.02	0.01	0.19	0.00	0.01	100.58
5	Ba-1	98.97	0.16	0.17	0.08	0.02	0.41	0.00	0.01	99.82
6	Ba-1	98.81	0.15	0.44	0.00	0.02	0.01	0.00	0.00	99.42
7	Ba-1	98.56	0.16	0.33	0.00	0.03	0.13	0.00	0.00	99.22
8	Ba-1	100.34	0.21	0.11	0.00	0.02	0.10	0.00	0.01	100.80
9	Ba-1	100.42	0.22	0.07	0.00	0.01	0.08	0.00	0.01	100.80
10	Ba-1	99.79	0.18	0.09	0.01	0.00	0.04	0.00	0.01	100.12
11	Ba-1	98.25	0.20	0.26	0.04	0.02	0.18	0.00	0.00	98.95
12	Ba-1	98.16	0.25	0.27	0.00	0.00	0.20	0.00	0.00	98.88
13	Ba-1	100.50	0.18	0.12	0.00	0.02	0.05	0.00	0.01	100.89
14	Ba-1	98.22	0.17	0.24	0.03	0.01	0.17	0.00	0.00	98.84
15	Ba-5	98.65	0.15	0.31	0.07	0.00	0.00	0.00	0.00	99.18
16	Ba-5	98.64	0.16	0.21	0.02	0.02	0.03	0.00	0.00	99.07
17	Ba-5	99.02	0.21	0.46	0.05	0.00	0.04	0.00	0.00	99.78
18	Ba-5	96.15	0.16	0.84	0.21	0.02	0.11	0.00	0.00	97.49
19	Ba-5	95.91	0.22	0.79	0.10	0.03	0.25	0.00	0.00	97.31
20	Ba-5	96.98	0.22	0.70	0.08	0.03	0.24	0.01	0.02	98.28
21	Ba-5	98.46	0.23	0.29	0.03	0.02	0.09	0.00	0.00	99.11
22	Ba-5	100.07	0.18	0.26	0.04	0.01	0.03	0.00	0.00	100.58
23	Ba-5	98.18	0.21	0.29	0.01	0.00	0.12	0.00	0.01	98.81
24	Ba-5	98.54	0.19	0.34	0.06	0.02	0.05	0.00	0.00	99.21
25	Ba-6b	96.34	1.14	0.15	0.16	0.29	1.70	0.00	0.03	99.81
26	CD-H1	97.15	0.23	0.53	0.23	0.01	0.34	0.00	0.01	98.51
27	CD-H1	96.69	0.21	0.41	0.24	0.03	0.44	0.00	0.03	98.04
28	CD-H1	94.72	0.14	0.92	0.39	0.02	0.41	0.00	0.02	96.63
29	CD-H1	97.24	0.19	0.43	0.27	0.01	0.48	0.00	0.02	98.63
30	CD-H1	97.15	0.16	0.57	0.22	0.01	0.41	0.00	0.01	98.54
31	CD-H1	95.13	0.17	0.75	0.26	0.02	0.49	0.00	0.01	96.82
32	CD-H1	97.38	0.22	0.32	0.16	0.03	0.39	0.00	0.01	98.50
33	CD-H1	97.65	0.22	0.47	0.30	0.02	0.43	0.00	0.02	99.11
34	CD-D1	98.23	0.49	0.72	0.38	0.02	0.61	0.01	0.02	100.48
35	CD-D1	98.11	0.52	0.68	0.39	0.04	0.61	0.00	0.01	100.36
36	CD-D1	99.11	0.28	0.41	0.13	0.03	0.84	0.00	0.01	100.81
37	CD-D1	98.56	0.23	0.35	0.07	0.03	0.45	0.00	0.01	99.71
38	CD-D1	99.61	0.30	0.31	0.14	0.03	0.80	0.00	0.01	101.20
39	CD-D1	98.68	0.98	0.65	0.38	0.02	0.63	0.00	0.01	101.35
40	CD-D1	97.31	1.73	0.48	0.29	0.01	0.71	0.00	0.02	100.55
41	CD-D1	96.92	0.97	0.59	0.22	0.02	0.55	0.00	0.00	99.28
42	CD-D1	93.93	3.09	0.68	0.41	0.05	0.63	0.00	0.02	98.80
43	CD-D1	99.34	0.24	0.25	0.12	0.01	0.69	0.00	0.01	100.66
44	CD-D1	98.33	0.34	0.45	0.11	0.05	0.73	0.00	0.01	100.02

Table 3c: Chemical composition of manganite (weight %).

No.	Sample	Mn_2O_3	Fe_2O_3	SiO_2	Al_2O_3	MgO	CaO	BaO	K_2O	Total
1	Ba-5-1	89.58	0.15	0.31	0.07	0.00	0.00	0.00	0.00	90.11
2	Ba-5-2	89.56	0.16	0.21	0.02	0.02	0.03	0.00	0.00	90.00
3	Ba-5-3	89.91	0.21	0.46	0.05	0.00	0.04	0.00	0.00	90.67
4	Ba-5-4	87.30	0.16	0.84	0.21	0.02	0.11	0.00	0.00	88.64
5	Ba-5-5	87.09	0.22	0.79	0.10	0.03	0.25	0.00	0.00	88.49
6	Ba-5-6	88.06	0.22	0.70	0.08	0.03	0.24	0.01	0.02	89.35
7	Ba-5-7	89.40	0.23	0.29	0.03	0.02	0.09	0.00	0.00	90.05
8	Ba-5-8	89.14	0.21	0.29	0.01	0.00	0.12	0.00	0.01	89.78
9	Ba-5-9	89.48	0.19	0.34	0.06	0.02	0.05	0.00	0.00	90.15

Table 4a: Chemical composition of the Jurassic shale with manganese mineralization (oxides in weight %, elements in ppm). Part 1 from 2.

No.	1	2	3	4	5	6	7	8	9	10	11	12	13	14	15	16	17	18	19	20	21	22	23
Sample	**Ba 1**	**Ba 4**	**Ba 5**	**Ba 6a**	**BaČD-H14**	**BaHN1-6A**	**BaL-4**	**BaMA-11**	**BaMA-12**	**BaSA-4**	**Dik 1**	**Dik 2**	**Dik 3**	**Dik 4**	**Dik 5**	**Dik 6**	**Dik 7**	**LR 2**	**LR 3**	**Ma-P-0m**	**Ma-P-1m**	**Ma-P-1.5–1.6m**	**Ma-P-2m**
SiO_2	7.74	16.55	25.31	37.99	23.56	15.22	37.13	39.24	38.10	29.50	22.03	31.30	39.24	25.20	9.20	46.00	11.68	13.95	8.35	41.78	39.16	23.21	29.14
TiO_2	0.22	0.21	0.43	0.20	0.37	0.19	0.15	0.61	0.53	0.41	0.057	0.069	0.253	0.093	0.389	0.194	0.191	0.34	0.10	0.688	0.546	0.181	0.320
Al_2O_3	2.47	3.02	6.03	3.87	7.25	3.22	5.39	12.62	11.86	9.10	1.41	1.45	4.95	1.81	4.41	5.50	4.96	5.06	1.23	14.07	11.65	4.50	7.00
FeO	1.14			6.73																			
Fe_2O_3	7.58			3.21																			
Fe_2O_3 total	8.85	16.18	11.22	10.68	7.60	14.38	9.94	4.95	5.16	9.38	0.98	2.35	3.28	1.90	11.29	6.94	13.09	15.23	2.91	5.61	5.00	2.97	3.79
MnO	22.84	24.66	21.14	3.66	13.81	20.94	2.62	0.21	0.18	15.24	2.054	2.299	1.870	2.305	33.22	15.70	31.12	34.06	3.08	0.160	0.170	0.283	0.234
MgO	3.75	1.87	1.76	5.26	3.09	1.87	6.37	3.07	2.43	1.97	1.07	0.67	2.06	0.92	2.39	1.93	2.53	0.96	9.79	3.06	2.70	1.45	2.03
CaO	22.95	15.93	9.06	16.01	16.40	14.85	16.52	17.79	19.76	10.85	40.22	34.14	25.27	37.21	10.52	7.57	12.31	5.76	37.49	15.04	18.98	36.07	29.62
Na_2O	0.02	0.53	0.68	0.09	0.69	0.64	0.92	1.38	1.29	1.21	0.07	0.05	0.04	0.06	0.08	0.64	0.08	0.24	0.59	0.64	0.63	0.35	0.59
K_2O	0.40	1.11	2.00	0.20	0.87	0.44	0.14	2.48	2.30	0.82	0.24	0.32	1.25	0.48	1.13	1.03	0.91	1.00	0.64	2.45	1.92	0.76	1.11
P_2O_5	0.61	0.42	0.21	0.22	0.13	0.39	0.53	0.10	0.10	0.32	0.08	0.20	0.20	0.12	0.73	0.58	0.92	0.24		0.16	0.17	0.10	0.13
H_2O-	0.65	1.85	0.90	0.34	0.18	0.34	0.08	0.07	0.03	0.46	0.25	0.35	0.36	0.29	2.23	1.84	3.68	8.50	0.07	0.51	0.43	0.29	0.33
***LOI**	29.72	17.30	20.92	19.68	25.73	27.14	19.84	17.07	17.90	20.34	31.67	27.08	21.38	29.75	26.44	13.71	22.06	14.51	35.66	16.12	18.78	29.80	25.74
B	164	48	118	16	33	38	<10	91	71	107								57	39				
Ba	245	<30	<30	66	102	53	<30	148	127	165	62	69	266	95	382	256	242	598	2119	308	256	101	152
Co	18	95	191	27	62	48	18	12	10	122	4	14	13	12	78	64	119	93	3	21	22	10	19
Cr	25	54	55	22	37	33	32	49	47	47	8	15	34	16	30	8	16	60	10	85	71	30	36
Cu	29	15	39	37	36	26	30	43	45	69	4	12	24	14	44	26	63	45	13	45	39	20	32
La				13							13	25	26	16	72	41	70			23	26	16	16
Mo				3							3	3	3	3	3	3	6	11		2	2	2	2
Ni	19	23	92	40	48	21	20	39	38	102	13	19	28	14	60	46	73	25	11	69	54	28	43
Pb	25	19	33	16	24	42	17	22	25	75	6	12	13	12	26	23	26	51	8	29	27	22	35
Sr	480	406	175	525	239	211	401	330	312	223	500	348	226	384	318	182	271	1000	500	1258	1484	2202	2254
V	28	34	41	38	87	70	75	117	103	104	11	20	43	39	82	63	71	83	63	121	77	61	45
Y		49	41	18	35	34	35	33	25	35	10	21	17	15	55	30	59	19		21	21	15	21
Zr		274	290	62	69	160	82	37	41	137	10	18	50	19	109	44	71	97		114	93	38	68
Th		11	13		9	10	4	10	9	12	3	4	5	3	14	7	14		4	10	8	7	10
U		3	3		3	2	3	2	2	3	2	2	2	2	4	2	6		2	3	3	3	3
TC%	8.55	7.65	5.82	5.93	8.86	8.76	6.55	4.52	4.4	5.35	7.35	6.27	5.03	7.02	6.12	3.61	4.8	0.32	11.05	4.02	4.95	8.37	6.9
TOC%	0.97	1.62	1.24	1.17	2.65	3.2	1.7	0.96	0.67	2.68	0.21	0.1	0.12	0.18	2.26	1.08	1.68	0.24	1.82	0.42	0.31	0.3	0.42
TIC%	6.58	6.03	4.58	4.76	6.21	5.56	4.85	3.56	3.73	2.67	7.14	6.17	4.91	6.84	3.86	2.53	3.12	0.08	9.23	3.6	4.64	8.07	6.48
CO_2 carb.		22.07	16.76	17.422	22.73	20.35	17.75	13.03	13.652	9.77	26.132	22.582	17.971	25.034	14.127	9.26				13.18	16.98	29.54	23.72

Table 4a: *Continued*. Part 2 from 2.

No.	24	25	26	27	28	29	30	31	32	33	34	35	36	37	38	39	40	41	42	43	44	45	46
Sample	**Ma-P-3m**	**Ma-P-3.4–3.43m**	**Ma-P-4m**	**Ma-P-5m**	**Ma-P-6m**	**Ma-P-7m**	**Ma-P-8m**	**Ma-P-8.10–8.16m**	**Ma-P-9m**	**Ma-P-9.5m**	**ŠJ 1**	**ŠJ 9**	**ŠJ-16**	**Za 1**	**Za 2**	**Za 6**	**Za 7**	**ZaK 9**	**ZaH-11**	**ZaH-19**	**ZaH-20**	**ZaH-21**	**ZaK-22**
SiO_2	38.16	27.22	38.17	36.88	34.64	39.08	43.69	23.21	38.72	31.31	33.12	27.94	32.87	4.55	10.43	35.05	19.82	33.15	49.12	34.5	15.44	39.21	7.23
TiO_2	0.566	0.144	0.528	0.519	0.568	0.539	0.730	0.137	0.566	0.372	0.18	0.13	0.12	0.04	0.04	0.19	0.18	0.25	0.41	0.15	0.174	0.286	0.128
Al_2O_3	12.24	3.54	11.01	11.17	12.97	11.43	15.73	3.45	12.01	8.14	8.41	2.72	2.01	0.60	0.75	3.23	2.62	4.12	11.56	2.81	2.62	6.57	2.87
FeO											2.56				2.18					7.78			
Fe_2O_3											2.38				3.49					3.282			
Fe_2O_3 total	4.77	2.34	4.78	4.67	4.99	4.15	4.62	2.60	5.10	5.07	5.22	23.29	20.08	5.00	5.91	9.96	35.67	14.81	8.34	11.93	2.85	16.67	14.23
MnO	0.176	0.255	0.181	0.190	0.174	0.166	0.132	0.271	0.163	0.209	18.27	20.59	29.72	9.11	8.03	13.17	9.16	11.69	0.68	14.20	2.498	6.069	24.66
MgO	3.00	3.21	2.46	2.67	3.04	2.59	2.91	1.13	2.67	1.97	0.94	1.51	0.15	9.69	8.32	2.55	1.75	2.36	1.74	2.59	8.75	3.04	4.61
CaO	18.97	32.80	20.77	21.24	20.49	19.91	13.39	37.77	19.28	27.52	19.11	1.89	1.31	31.65	29.34	20.64	11.16	17.91	10.68	9.25	30.82	8.22	11.85
Na_2O	0.66	0.42	0.64	0.65	0.86	0.73	0.87	0.37	0.72	0.56	0.02	0.88	0.86	0.11	0.29	0.10	0.34	0.10	0.74	0.18	0.24	0.32	0.11
K_2O	2.06	0.58	1.92	1.80	2.09	1.98	2.76	0.51	1.98	1.34	0.03	0.81	0.80	0.07	0.08	1.33	1.06	1.72	5.52	0.53	0.36	1.06	0.42
P_2O_5	0.18	0.07	0.15	0.16	0.16	0.16	0.22	0.07	0.18	0.11	2.56	0.03	0.04	0.10	0.51				0.28	0.16	0.38	0.89	1.09
H_2O-	0.32	0.26	0.35	0.34	0.33	0.38	0.49	0.30	0.41	0.29	0.01	0.51	2.09	0.10	0.03	0.05	0.19	0.15	0.30	0.56	0.36	1.31	0.75
***LOI**	18.93	29.20	19.17	19.84	19.77	18.99	14.74	30.21	18.36	23.02	14.56	19.30	9.52	38.67	36.72	13.39	17.61	13.47	10.17	21.05	35.60	17.39	32.68
B											2	357	41	36	38	52	42	151	113	82			
Ba	276	81	237	235	268	255	350	75	252	187	15	127	42	1100	1286	20	20	63	119	398	1133	220	839
Co	19	7	19	15	19	27	19	7	18	19	106	30	21	6	14	21	65	19	31	45	9	34	68
Cr	67	27	68	69	72	68	93	30	70	50	24	23	59	7	4	35	15	46	58	26	24	17	3
Cu	45	16	41	44	49	45	56	21	51	34	2	17	31	12	7	32	47	62	84	30	26	51	25
La	30	12	27	18	26	32	27	9	28	22	61					186	82	151		24	14	49	45
Mo	2	2	2	2	2	2	2	2	2	2	13					4	4	6		–3	7	3	3
Ni	72	19	45	54	58	45	60	24	56	51	58	48	20	4	5	19	108	31	42	34	25	44	36
Pb	38	19	24	29	24	23	24	19	25	30	38	21	45	7	11	14	8	22	41	26	11	27	14
Sr	1426	2750	1392	1542	1449	1240	863	2384	1339	1665	227	192	>500	500	416	316	136	427	291	600	930	508	586
V	94	38	84	87	92	91	120	35	95	64	50	17	20	3	11	47	12	59	221	53	253	77	45
Y	19	18	20	19	16	18	21	15	24	21	18	37	31			79	22	98	46	22	16	66	44
Zr	93	33	89	90	93	93	116	27	90	70	58	220	184			42	86	81	73	37	41	63	35
Th	10	6	9	10	10	9	12	7	10	10		11	11	2	2		4		8		3	7	11
U	3	3	3	3	3	3	3	3	3	3		2	2	2	2		2		2		2	2	2
TC%	4.98	8.55	5.05	5.26	5.38	5.42	4.5	8.27	4.8	6.54	4.56	5.11	0.12	11.62	11.02	6.88	3.23	6.42	6.18	6.61	9.30	4.87	8.68
TOC%	0.47	0.28	0.46	0.47	0.4	0.58	0.56	0.52	0.57	0.38	0.1	0.2	0.12	0.5	0.44	1.2	0.57	1.74	3.56	4.42	1.73	2.78	2.92
TIC%	4.51	8.27	4.59	4.79	4.98	4.84	3.94	7.75	4.23	6.16	4.46	4.91	st.	11.12	10.58	5.68	2.66	4.68	2.62	2.19	7.57	2.09	5.76
CO_2 carb.	16.51	30.27	16.80	17.53	18.23	17.71	14.42	28.37	15.48	22.55		17.97	st.						9.58	8.015	27.706	7.649	21.08

Table 4b: Chemical composition of the Paleogene shale with manganese mineralization (oxides in weight %, elements in ppm). Part 1 from 2.

No.	1	2	3	4	5	6	7	8	9	10	11	12	13	14	15	16	17	18	19	20	21	22	23	24	25	26	27	28	29	30	31
Sample	**By-1**	**By-2**	**By-3**	**By-P-0**	**By-P-1**	**By-P-2**	**By-P-3**	**By-P-4**	**By-P-5**	**By-P-6**	**By-P-7**	**By-P-8**	**By-P-9**	**By-P-9.40**	**By-P-9.50**	**By-P-10**	**By-P-11**	**By-P-11.10**	**By-P-12**	**By-P-13**	**By-P-14**	**By-P-15**	**By-P-16**	**By-P-17**	**By-P-18**	**By-P-19**	**Ho 1**	**Ho 3**	**Kis 1**	**Kis 2**	**Kiš 12**
SiO_2	28.05	25.08	32.87	36.68	31.19	30.06	25.28	38.53	29.81	35.79	36.02	17.91	41.43	42.84	24.48	34.49	23.99	36.02	38.76	40.65	34.51	44.92	36.25	45.62	43.66	39.05	3.42	3.66	12.11	22.27	30.69
TiO_2	0.25	0.14	0.43	0.53	0.39	0.36	0.34	0.56	0.30	0.53	0.56	0.16	0.55	0.63	0.13	0.45	0.26	0.50	0.52	0.63	0.43	0.60	0.48	0.70	0.70	0.52	0.13	0.07	0.19	0.31	0.34
Al_2O_3	7.63	5.85	8.90	11.24	8.35	8.31	9.60	11.52	4.97	10.91	11.53	2.81	11.85	14.14	4.27	9.17	7.04	10.59	11.25	13.77	8.55	12.33	10.94	15.14	14.22	10.59	1.88	1.57	2.72	4.67	5.12
FeO																												0.73	0.87	1.53	2.18
Fe_2O_3																												1.69	1.48	1.77	1.69
Fe_2O_3 total	18.15	25.27	6.84	5.12	6.19	5.70	19.59	9.43	4.59	5.95	6.16	3.68	9.01	10.83	25.28	8.92	11.93	7.56	8.74	10.09	7.97	7.09	12.40	6.15	5.57	11.61	4.11	2.50	2.45	3.47	4.11
MnO	16.05	13.13	1.10	0.50	1.00	1.29	11.59	1.22	1.28	0.53	0.51	1.31	0.65	2.40	14.09	1.77	29.68	0.65	0.74	1.29	0.94	0.41	0.49	0.50	0.45	1.33	29.15	28.04	29.88	14.04	15.96
MgO	1.71	1.90	1.45	1.79	1.38	1.33	2.34	2.27	1.13	1.67	1.78	1.08	1.95	2.46	1.34	1.83	1.60	1.68	1.71	2.31	1.45	1.93	1.80	2.13	1.91	1.62	2.65	2.96	5.26	3.51	3.25
CaO	10.40	11.04	23.61	20.78	24.98	25.96	12.20	16.11	30.10	21.56	20.36	39.66	14.96	9.64	11.91	20.45	8.19	19.93	16.98	12.49	22.36	14.09	16.37	11.75	14.11	15.53	23.42	26.40	15.20	23.66	15.06
Na_2O	0.21	0.09	0.54	0.51	0.39	0.39	0.22	0.53	0.66	0.52	0.52	0.28	0.55	0.55	0.07	0.47	0.18	0.51	0.55	0.62	0.55	0.64	0.40	0.63	0.66	0.53	0.08	0.10	0.07	0.33	0.60
K_2O	0.79	0.28	1.62	2.23	1.65	1.67	1.01	1.91	0.83	2.15	2.27	0.47	2.02	2.43	0.29	1.45	0.84	2.08	2.09	2.29	1.61	2.23	1.98	3.13	3.02	1.91	0.57	0.41	0.49	0.93	0.92
P_2O_5	1.00	1.31	0.18	0.23	0.19	0.15	2.56	0.20	0.16	0.15	0.15	0.36	0.27	0.14	1.16	0.23	0.39	0.20	0.16	0.18	0.33	0.21	0.18	0.22	0.17	0.24	0.11	0.17	0.18	0.19	0.20
H2O-	4.86	4.36	1.61	1.32	1.23	1.21	4.16	1.92	0.75	1.51	1.59	0.62	2.07	2.99	3.98	1.92	5.51	1.57	1.76	2.57	1.42	1.77	2.02	1.58	1.62	2.00	0.08	0.43	0.32	0.16	0.53
LOI	15.05	15.44	22.19	20.03	23.94	24.42	14.96	17.53	25.91	20.07	19.95	31.96	16.56	13.70	16.74	20.47	15.50	19.99	18.32	15.45	21.08	15.30	18.40	13.77	15.28	16.83	34.05	33.06	31.03	26.43	22.74
B																											120	77.00	245	231	75
Ba	1354	600	276	263	251	327	750	339	250	285	290	153	299	386	432	308	1304	284	392	483	307	349	326	458	426	491	245	199	150	265	241
Co	58	65	30	8	20	21	88	56	9	19	19	12	28	68	56	32	35	33	22	39	25	26	71	19	15	34	7	3	4.00	12	7
Cr	85	59	79	97	90	94	91	113	51	112	116	30	122	134	61	88	110	121	107	123	92	107	155	116	105	130	28	35	71	73	41
Cu	50	32	47	36	63	56	47	55	15	48	57	11	57	82	30	54	47	57	57	71	59	55	72	43	41	63	20	12	22	34	12
La	29	32	28	24	22	22	65	34	18	26	28	13	33	30	30	27	29	29	29	34	28	30	33	30	30	33		9			16
Mo	10	7	3	2	2	5	5	2	2	2	2	2	2	2	2	2	19	2	2	2	4	2	3	2	2	4		15			–3
Ni	92	90	60	51	62	64	148	123	38	63	66	34	87	156	81	106	83	95	76	118	69	90	136	76	62	113	29	13	21	41	30
Pb	10	3	18	25	20	21	16	32	17	20	20	11	24	31	3	19	10	24	18	26	21	26	38	28	27	27	28	7	27	18	12
Sr	1000	701	879	708	1139	1147	897	690	1112	789	770	1069	664	437	723	987	1051	807	669	510	796	513	760	446	524	611	457	733	316	450	363
V	112	85	114	143	163	132	176	164	48	149	167	34	159	234	76	155	147	198	182	194	165	154	274	180	168	192	36	42	77	62	52
Y	31	35	23	25	20	19	78	27	18	24	27	11	36	25	39	30	36	29	30	30	34	30	33	27	28	31		8			15
Zr	57	38	87	100	72	66	77	133	101	111	108	39	117	122	32	101	46	100	103	132	106	133	89	133	135	116		19			103
Th	8	10	8	10	8	9	9	11	5	9	9	4	11	13	8	8	10	9	10	10	9	9	8	12	10	10	5			7	
U	4	2	5	3	8	5	5	3	5	3	3	3	6	3	3	3	3	5	7	3	5	5	3	5	5	3	2			2	
TC%	1.56	1.92	6.1	4.93	7.47	5.93	1.71	4.43	7.04	5.1	4.94	8.61	3.68	2.62	1.75	4.8	1.05	5.45	4.89	3.51	5.31	3.7	4.62	3.17	3.52	3.71	10.52	10.78	9.03	7.92	6.83
TOC%	0.37	0.39	0.97	0.62	1.25	0.96	0.48	1.08	0.42	0.56	0.63	0.2	0.85	1.04	0.53	0.94	0.58	0.93	1.07	1.1	0.75	0.84	1.14	0.59	0.67	0.73	0.4	2.12	0.55	0.53	2.65
TIC%	1.19	1.53	5.13	4.31	6.22	4.97	1.23	3.35	6.62	4.54	4.31	8.41	2.83	1.58	1.22	3.86	0.47	4.52	3.82	2.41	4.56	2.86	3.48	2.58	2.85	2.98	10.12	8.66	8.48	7.39	4.18
CO_2 carb.	4.36	5.60	18.78	15.78	22.77	18.19	4.50	12.26	24.23	16.62	15.78	30.78	10.36	5.78	4.47	14.13	1.72	16.54	13.98	8.82	16.69	10.47	12.74	9.44	10.43	10.91		31.70			15.30

***LOI** — loss of ignition.

Table 4b: *Continued*. Part 2 from 2.

No.	32	33	34	35	36	37	38	39	40	41	42	43	44	45	46	47	48	49	50	51	52	53	54	55	56	57	58	59	60	61	62
Sample	**Kiš 15**	**Kiš 16**	**Ko 1**	**Mich 8**	**Mich 9**	**Mich 11**	**OBP-1**	**OBP-2**	**P-1**	**P-2**	**P-3**	**P-4**	**P-5**	**P-6**	**P-7**	**P-8**	**P-9**	**P-10**	**P-11**	**P-12**	**P-13**	**Pu 11-R1**	**Pu 11-R2**	**P11-6**	**P11-7**	**Ra-2**	**St-1**	**St-5**	**Šv 2**	**Šv 7**	**Šv 8**
SiO_2	9.84	12.27	23.19	8.42	12.04	8.09	8.86	14.10	34.34	34.35	27.41	31.93	32.49	39.53	49.99	36.16	36.07	34.17	35.52	35.20	40.19	13.18	37.25	27.47	25.89	35.82	49.22	13.19	4.19	9.34	20.37
TiO_2	0.08	0.31	0.51	0.39	0.34	0.09	0.156	0.245	0.44	0.43	0.38	0.45	0.45	0.54	0.67	0.51	0.51	0.46	0.53	0.47	0.63	0.12	0.49	0.32	0.20	0.482	0.40	0.20	0.10	0.08	0.25
Al_2O_3	1.74	6.76	8.71	4.53	4.33	1.97	3.07	4.55	9.70	9.47	8.50	9.05	10.13	11.44	17.12	11.15	11.24	10.33	10.44	10.43	12.97	3.37	10.06	7.35	4.25	10.14	7.89	5.03	1.58	1.74	4.90
FeO	0.87	0.00	0.69			2.98																								0.22	2.25
Fe_2O_3	1.75	7.15	8.09			3.23																								2.638	1.61
Fe_2O_3 total	2.72	7.15	8.86	5.42	9.36	6.54	2.90	3.25	3.82	3.90	3.27	3.61	3.79	4.61	5.68	4.42	5.05	3.93	5.11	7.80	6.17	21.94	8.77	12.55	2.66	10.28	2.16	20.74	2.20	2.88	4.10
MnO	33.01	39.74	34.30	43.23	33.97	30.54	0.19	0.37	0.06	0.05	0.08	0.04	0.06	0.20	0.19	0.39	0.31	0.74	0.86	1.21	0.21	8.52	1.63	4.44	1.27	5.95	0.96	25.70	21.65	32.57	22.38
MgO	2.05	1.55	0.55	1.85	1.50	3.61	14.91	11.78	1.90	1.98	2.10	2.98	2.59	1.76	2.22	1.67	1.72	1.52	1.68	2.39	1.73	5.67	2.46	2.97	2.56	1.38	1.04	1.35	3.66	2.20	4.08
CaO	17.84	12.37	2.29	8.81	9.63	15.76	28.56	28.16	24.68	24.92	29.64	25.30	24.63	19.84	9.02	21.03	21.73	24.11	21.77	19.75	16.74	15.48	17.89	19.64	33.16	16.03	17.11	12.87	30.41	18.02	14.87
Na_2O	0.08	0.17	0.57	0.10	0.12	0.13	0.14	0.19	0.62	0.62	0.43	0.56	0.53	0.68	0.79	0.68	0.67	0.73	0.57	0.68	0.64	0.09	0.77	0.38	0.88	0.51	2.37	0.10	0.48	0.06	0.09
K_2O	0.33	1.12	1.68	3.30	3.11	0.48	0.64	0.95	1.93	1.84	1.77	1.85	2.04	2.11	2.92	2.08	2.00	1.84	2.16	1.84	2.56	0.22	1.47	1.04	0.48	1.54	1.22	0.75	0.54	0.36	1.08
P_2O_5	0.15	0.35	0.17	0.10	0.24	0.31	0.11	0.11	0.06	0.09	0.07	0.08	0.06	0.10	0.14	0.11	0.11	0.14	0.12	0.17	0.12	0.76	0.16	0.25	0.10	0.24	0.14	1.22	0.08	0.14	0.16
H2O-	0.40	6.15	4.03	5.77	7.81	0.77	0.64	0.90	1.45	0.15	1.36	1.36	1.51	1.83	3.03	1.80	1.71	1.84	1.47	1.58	1.31	0.73	2.01	1.30	0.47	3.59	0.14	5.26	0.10	0.48	0.86
LOI	30.81	17.82	14.89	17.62	17.20	32.14	40.28	36.15	22.20	22.19	26.30	23.96	23.03	18.86	11.18	21.68	20.42	21.74	20.93	19.82	17.87	30.34	18.37	23.43	28.44	17.39	16.95	18.73	34.70	30.95	27.08
B	114	37	26	10	19	52																					19		139	90	125
Ba	190	271	30	<30	<30	215	336	202	279	321	254	823	309	291	284	260	246	300	406	275	483	222	266	178	74	1073	229	411	241	211	160
Co	4	13	34	34	22	5	2	5	7	9	4	5	14	10	12	11	16	7	16	26	15	46	51	42	4	26	5	49	8	12	16
Cr	46	61	144	74	60	22	33	48	52	42	42	45	49	63	75	62	57	59	77	63	76	40	64	31	24	93	24	94	28	47	115
Cu	18	20	59	14	10	6	11	14	34	32	36	24	36	38	58	40	40	38	44	40	35	14	43	35	10	36	17	33	21	14	43
La	9	25	83			13	9	14	25	26	24	24	25	27	39	27	26	25	25	26	27	20	28	23	10	24		25		10	17
Mo	10	–3	81			–3	2	2														2	2	3	3	6		2		52	–3
Ni	35	71	186	44	18	14	16	29	28	26	20	26	36	48	46	47	50	27	56	55	57	81	94	102	22	70	8	98	18	73	67
Pb	5	19	36	43	39	8	9	10	–5	6	6	3	12	12	16	8	10	6	12	3	20	3	19	15	10	21	10	7	25	14	14
Sr	621	836	338	>500	>500	329	396	286	625	643	625	603	558	576	330	663	665	754	787	701	465	709	634	612	695	649	218	637	383	482	420
V	55	100	177	61	30	27	35	74	79	65	60	73	80	89	118	92	86	87	123	98	103	66	103	85	36	119	49	118	36	62	146
Y	7	27	37	19	18	13	8	14	18	20	18	19	18	20	24	20	19	19	19	20	21	19	22	18	8	22	21	32		8	15
Zr	18	61	114	114	299	22	34	64	90	83	64	81	82	101	140	96	88	79	89	80	121	26	104	58	45	97	72	40		18	49
Th				14	17		2	4														7	9	6	3	9	8	12	4		
U				2	3		3	3														2	4	2	2	3	2	9	2		
TC%	9.57	1.71	0.24	0.12	0.51	9.72	11.13	9.78														8.96	4.12	5.38	6.96	3.03	4.27	1.74	10.78	9.55	7.8
TOC%	3.34	1.25	0.24	0.005	0.1	4.65	0.2	0.27														5.27	0.92	1.36	0.17	0.52	0.63	0.45	0.42	2.93	2.06
TIC%	6.23	0.46	0	0.12	0.41	5.07	10.93	9.51														3.69	3.2	4.02	6.79	2.51	3.64	1.29	10.36	6.62	5.74
CO_2 carb.	22.80	1.68		0.44	1.50	18.56	40.00	34.81														13.51	11.71	14.71	25.47	9.19	13.32	4.72		24.23	21.01

***LOI** — loss of ignition.